

Mathias Lien

Design of Topology Optimized Titanium Brake calipers

For racing application

Bachelor's project in Mechanical Engineering

Supervisor: Evangelos Tyflopoulos

May 2020



Nova (2019)

Mathias Lien

Design of Topology Optimized Titanium Brake calipers

For racing application

Bachelor's project in Mechanical Engineering
Supervisor: Evangelos Tyflopoulos
May 2020

Norwegian University of Science and Technology
Faculty of Engineering
Department of Mechanical and Industrial Engineering



**DESIGN OF
TOPOLOGY OPTIMIZED
TITANIUM BRAKE CALIPERS
- FOR RACING APPLICATIONS**

REPORT BACHELOR THESIS

Title:

- Design of Topology Optimized Titanium Brake Calipers (for racing applications)
- Design av Topologi Optimalisert Titan Bremskaliper (for motorsport)

Project number

MTP-K-2020-08

Author(s)

- Mathias Lien

Company (external)

- DMG Mori, Germany

Supervisor NTNU

- Evangelos Tyflopoulos

Report is CLOSED

Date: 19.05.2020

The braking system of a Formula Student race car requires high resistance to heat and dynamic loads. The brake caliper, which consists of two or more brake pads, applies a friction force to the brake disc to stop the vehicle. The purpose of this thesis is to design a braking system, with focus on the brake caliper, for Revolve NTNU's 2020 Formula Student race car, reducing overall system weight and volume, with similar or improved performance.

Bremsesystemet til en Formula Student racing bil krever høy motstand mot varme og dynamiske laste. Bremskaliperen, som består av to eller flere bremsklosser, påfører en friksjonskraft på bremseskiven for å stoppe kjøretøyet. Formålet med denne oppgaven er å designe et bremsesystem, med spesielt fokus på bremskaliperen, til Revolve NTNU's 2020 Formula Student racing bil, med formål om å redusere total systemvekt og volum, med lignende eller forbedret ytelse.

Stikkord: Bremskaliper, Topologi Optimalisering, Additiv Produksjon, Formula Student, Mekanisk, Ingeniørvitenskap, Kjøretøy

Keywords: Brake Caliper, Topology Optimization, Additive Manufacturing, Formula Student, Mechanical, Engineering Science, Automotive

Preface

This bachelor thesis is a culmination of three years of study in mechanical engineering, written on behalf of Revolve NTNU. The task in hand, was to conceptualize, develop and design a brake system for Revolve NTNU's 2020 open-wheel racing car. I have always had a burning passion for race cars and advanced mechanical engineering. Revolve NTNU gave me the opportunity to work in a fast-paced environment, working with race car technology and writing my bachelor thesis on the project. For that I am very grateful!

The findings of this thesis were initially to be presented at SAP NOW in Oslo on March 19th but was cancelled by the recent development of the COVID-19 pandemic.

A lot of committed people and companies have been hugely helpful and an absolute necessity to be able to carry out this thesis. I would like to thank NTNU and the Department of Mechanical Engineering for helping Revolve NTNU as an organization, but also student individuals, facilitating projects like Revolve. This inspires us to work harder to realize our career dreams and further expand our engineering competence. On behalf of myself and Revolve NTNU, I would like to thank some of the sponsors that have contributed to this project: SAP and SIMULIA for providing software and economic assistance; DMG Mori, Trondheim Stål, SEAL Engineering and SINTEF IPK for manufacturing, machining and technical guidance on the project; and PLM Technology giving us the necessary simulation software and assistance throughout the project. I would also like to thank Revolve NTNU, entrusting me with the daunting task of designing a brake system for their 2020 race car. I also want to thank Alumni for giving me the necessary guidance to finish the project.

This thesis will address mechanical and automotive engineering knowledge, material science, load case calculations, test result analysis, concept development, design optimization, finite element analyses and production processes. For readers, general knowledge about these topics are recommended.

Abbreviations

| | |
|-----------------|--|
| AM | – Additive Manufacturing |
| CAD | – Computer-Aided Design |
| CAE | – Computer-Aided Engineering |
| CNC | – Computer Numerical Control |
| FEA | – Finite Element Analysis |
| FS | – Formula Student |
| GD&T | – Geometric dimensioning and tolerancing |
| KERS | – Kinetic Energy Recovery System |
| NTNU | – Norwegian University of Science and Technology |
| SAE | – Society of Automotive Engineers |

Summary

The braking system of a Formula Student race car requires high resistance to heat and dynamic loads. The brake caliper is a hydraulic component designed to apply a friction force between the brake disc and brake pad, to stop the vehicle. This is done according to the drivers input on the brake pedal.

Our formula student competitors often buy commercial units from external suppliers, adapting designs from other racing disciplines into their own. Consequently, accepting compromises such as added weight, challenges with integration and possibly a sacrifice in function.

The purpose of this thesis is to design a braking system for Revolve NTNU's 2020 formula student race car, with the goal of reducing overall system weight and volume, while maintaining similar or improved performance. The load case for the brake caliper will be based on a combination of simplified vehicle models, calculations and live data seen through Revolve NTNU's own data monitoring software, Revolve Analyze. The caliper design is outlined by topology optimized geometry from TOSCA and Discovery Live, adapted to be produced using a combination of additive and traditional manufacturing methods. For verification of the final designs, the Abaqus/CAE FEM software will be utilized. The simulations would then be compared to test results from mechanical testing and validated on the vehicle during summer testing and competitions. Because of the redesign of the calipers, unsprung mass from the suspension have been reduced by over 50% compared to commercial caliper and a weight decrease of almost 10 percent in compared to the 2019 brake calipers.

Sammendrag

Bremsesystemet til en Formula Student racerbil krever høy motstand mot varme og dynamiske belastninger. Bremsekaliperen, som består av to eller flere bremseklosser, påfører en friksjonskraft på bremseskiven for å stoppe kjøretøyet i henhold til hvor hardt føreren trykker på pedalen. Våre konkurrenter i Formula Student kjøper ofte kommersielle enheter fra eksterne leverandører, og tilpasser sine egne designs etter disse. Det betyr at man ofte må inngå kompromisser i form av økt vekt, utfordringer med implementering og generell funksjon av systemet.

Hensikten med denne oppgaven er å designe et bremsesystem for Revolve NTNUs 2020 Formula Student bil, med redusert systemvekt og lignende eller forbedret ytelse. Belastningene på bremsekaliperen vil være basert på en kombinasjon av forenklete kjøretøymodeller, beregninger og livedata fra Revolve NTNUs egne monitorsoftware program, *Revolve Analyze*. Kaliperen er designet for en kombinert produksjon av additive og tradisjonelle produksjonsmetoder, modellert etter topologioptimalisert geometri hentet fra TOSCA. Abaqus/CAE ble brukt for validering av det endelige designet. Simuleringene vil deretter bli sammenlignet med testresultater fra mekanisk testing og validert på kjøretøyet under testing. På grunn av redesignet av bremseene, har den unsprung massen fra suspensjonen blitt redusert med over 50% og redusert volumet fra tykkelsen med 44% sammenlignet med kommersielle bremser. Det er også spart opp mot 10% total vekt fra bremsekaliperene i 2019.

Table of Contents

| | |
|--|----|
| Preface..... | 2 |
| Abbreviations | 3 |
| Summary | 4 |
| Sammendrag | 5 |
| Table of Contents | 6 |
| 1 Introduction | 8 |
| 1.1 Background..... | 8 |
| 1.2 Purpose and Scope | 9 |
| 1.3 Thesis Objectives | 10 |
| 1.4 Approach and Limitations | 10 |
| 2 Theory | 11 |
| 2.1 Brake System Kinetics..... | 11 |
| 2.2 Thermodynamics | 13 |
| 2.3 Vehicle Dynamics..... | 15 |
| 2.4 Topology Optimization | 17 |
| 2.5 Additive Manufacturing..... | 18 |
| 2.6 Materials..... | 19 |
| 3 Brake Caliper and Load Case..... | 22 |
| 3.1 The Brake Caliper | 22 |
| 3.2 Load Case Analysis and KERS..... | 23 |
| 4 Brake Caliper Design | 26 |
| 4.1 Learning from previous calipers in Revolve | 26 |
| 4.1.1 Benchmark Caliper Testing..... | 28 |
| 4.2 Design Space..... | 29 |
| 4.3 Topology Optimization Setup | 29 |
| 4.3.1 ANSYS Discovery Live..... | 31 |
| 4.4 Topology Optimization Results..... | 32 |
| 4.5 Geometry Reconstruction | 34 |
| 4.6 Final Caliper Design | 34 |

| | | |
|-----|---|----|
| 4.7 | FEM Validation | 36 |
| 4.8 | FEM Results | 37 |
| 5 | Production..... | 39 |
| 5.1 | Manufacturing..... | 39 |
| 5.2 | Geometric Dimensioning and Tolerancing..... | 40 |
| 5.3 | Assembly..... | 41 |
| 5.4 | Mechanical Testing..... | 42 |
| 6 | Discussion..... | 43 |
| 7 | Conclusion..... | 45 |
| | List of Figures..... | 46 |
| | List of Tables..... | 47 |
| | Bibliography..... | 48 |
| | Appendix A | 51 |
| | Appendix B | 56 |
| | Appendix C..... | 62 |
| | Appendix D | 64 |
| | Appendix E..... | 66 |
| | Appendix F..... | 68 |

Chapter 1

1 Introduction

The first chapter will describe the background and motivation of the thesis, i.e. Formula Student competitions and Revolve NTNU and a description of the thesis objectives.

1.1 Background

Formula Student

Formula student or FSAE (Society of Automotive Engineers) is one of the largest competitions in the world for engineering students, organized by SAE International. The competition was first held in Texas in 1981, and in 1998 the first European competition was held in the UK. Currently, the competitions are now held in Spain, Netherlands, Italy, Austria, and Germany, to mention a few. The objective of the competition is to challenge teams of university undergraduates and graduates to conceptualize, design, develop, fabricate, and compete with a small single seater, open wheel race car. Teams are judged in static and dynamic events. Static events are an accumulation of the team's engineering work, both in compliance with the regulations and good engineering practices, done by former or present motorsport/automotive engineers. The teams are judged through technical inspection, cost and manufacturing, engineering design and business plan presentation. Dynamic events are performance competitions, driving disciplines like skid-pad, acceleration, autocross, endurance, and energy efficiency.

Revolve NTNU

Revolve NTNU is a student organization established by a group of students in the Norwegian University of Science and Technology in 2010. Since 2012 the organization has built a Formula Student race car every year. Revolve NTNU built the first electric race car (2014) in Norway, followed by the first 4-wheel driven electric race car (2016) in Scandinavia. In 2018 Revolve built their first autonomous race car and won the overall second place in Formula Student Germany with their electric race car.

1.2 Purpose and Scope

Based on the achievements that the 2018- and 2019 team has delivered the last two years, the expectations for the 2020 team has grown to be even greater. The basis of this thesis will be data we have available from the 2019 car and estimations for the 2020 car. A huge increase in sensors on the previous cars, making a lot of real-world data available. The completely revamped drivetrain from 2019, with in-house designed PMSM motors and motor controllers, will be kept for the 2020 season, also giving more consistent dynamic load and design parameters for the braking system with regards to KERS and design space.

This thesis will show the potential of an additively manufactured brake caliper design from titanium (Ti6Al4V), compared to commercially available systems and previous systems in revolve. Amongst Revolve NTNU's goals for 2020, one is to expand the traction circle. One of the most critical factors to improve performance by expanding the traction circle of a race car, is reducing overall vehicle mass and compliance in mechanical systems. As well as fulfilling these performance demands, production, machinability, assembly, practicality, and serviceability will have influence on the final design. The brake system is a part of the unsprung mass of the vehicle, which is important to minimise. High unsprung mass will increase the frequency length of the suspension's travel. This mean that the wheel stays up in the air for longer, resulting in less tire traction and less predictable handling characteristics, Claude Rouelle (2018). This leads engineers to pursue the balance of low weight designs, without sacrificing performance.

The brake system is a part of the suspension assembly and is interacting with the upright, gearbox and monocoque. For 2020, the suspension points have been modified, resulting in new design spaces for the both the uprights and brake calipers.

1.3 Thesis Objectives

The main objectives of this thesis are:

1. To describe different loading conditions and scenarios through calculated load cases and compare to live vehicle data.
2. To compare and evaluate the most suitable materials for a FS brake system with regards to temperature and performance.
3. To design a brake caliper with regenerative topology optimization design and validation with FEM software.
4. To produce sufficient technical drawings for production, in accordance with GD&T standards

1.4 Approach and Limitations

Based on live vehicle data from Nova (2019) and preliminary data for the 2020 car, calculations were carried out to describe the load case for the brake system, particularly the brake caliper. CAD-models are 3D modelled in SolidWorks and imported into Abaqus/TOSCA for topology optimization. The finished design will be tested through the finite element method (FEM) in Abaqus/CAE.

The brake system of the 2020 car have been 3D printed in parallel with the writing of this thesis. However, with the current development of the COVID-19 virus, Revolve NTNU has decided to stop all production for this year's car. This is a consequence of sponsors needing to back down from production, as well as competitions organized by the SAE have been cancelled. This thesis will be limited to development, design, and manufacturing of the brake calipers, as well as test jig design setup and approach.

Chapter 2

2 Theory

Chapter 2 will go further into the physics of braking, with focus on caliper kinetics and thermal calculations. This is followed by an introduction to some basic vehicle dynamic principles, topology optimization and material science.

2.1 Brake System Kinetics

An automotive brake system's main job is to slow down the mass of the vehicle through an applied friction force. Simply speaking, this involves a conversion of energy from the kinetic energy of the vehicle to thermal energy absorbed by the brake system. This can be expressed through the equation:

$$\frac{1}{2}m_v v_v^2 \rightarrow m_{BS} c_{h,BS} \Delta T_{BS}$$

Where:

| | |
|--------------|--|
| m_v | mass of the vehicle |
| v_v | velocity of the vehicle |
| m_{BS} | mass of the brake system |
| $c_{h,BS}$ | specific heat capacity of the brake system |
| ΔT_v | temperature change in the brake system |

In real world circumstances several of the suspension's components, including its surroundings, will distribute the absorbed energy between them. However, with this equation we have described the basic relation between a mass with a given velocity, and the difference in temperature of the absorbing system.

If the braking system is to be able to stop a moving vehicle, the calipers will need to apply a sufficient clamping force to the brake discs. The clamping force from the caliper translates to a friction force opposing disc's rotational direction. Assuming a constant friction coefficient, this can be expressed through the equation:

$$F_{friction} = F_{clamping} \times \mu \left(= \frac{M_b}{(\mu \times r_{eff})} \times \mu \right)$$

Where:

| | |
|----------------|---|
| $F_{friction}$ | Friction force on one wheel |
| $F_{clamping}$ | Clamping force |
| M_b | Brake torque on one wheel |
| r_{eff} | Effective pad radius |
| μ | Friction coefficient between pad and disc |

The pad friction coefficient will of course vary according to applied pressure, temperature, and surface roughness connected to wear.

As the brake system, in particular brake discs and calipers, interact with other systems such as the wheel hub and upright, the moment of the disc is assumed constant throughout the rotating wheel assembly. In a real-world scenario, other components of the wheel assembly will absorb loads during braking. To fully exploit a braking system's capabilities, the tire should be the limiting factor. Accordingly, both front and rear axle should be on the verge of locking. This can be expressed with:

$$m_v g \mu_{tire} = T_{limited} = m_v g z$$

Where:

| | |
|---------------|--|
| $T_{limited}$ | max wheel torque, given by the tire-ground friction coefficient and vehicle weight |
| z | deceleration proportional with g |
| μ_{tire} | friction coefficient between tire and ground. |

The equation above describes maximum negative acceleration, without exceeding μ_{tire} . As expected deceleration is 3.1 g , special tire compounds are needed accomplish this. In addition to the wheel torque, contributions to braking can be found with aerodynamic drag varying with speed; drivetrain losses such as bearing resistance, gear meshing and oil viscosity; and rolling resistance. [Advanced Vehicle Technology, Heinz Heisler]

2.2 Thermodynamics

The average braking energy q_0 of a moving vehicle, assuming constant braking over the entire process is given by [Advanced Vehicle Technology, Heinz Heisler]:

$$q_0 = \frac{(1 - s)(v_1 - v_2)m_v a}{2}$$

Where:

- s tire slip, ratio of difference between vehicle forward speed and circumferential tire speed
- a vehicle deceleration

Continued braking temperature development differ from single stop braking applications. According to research [Ceramic Matrix Composites: Fiber Reinforced Ceramics and their Applications] and theoretical investigations, approximately 90 to 95 percent of heat generation during braking is absorbed by the brake disc, assuming little to no heat dissipation. The last 5 to 10 percent of this heat is distributed through the pads, pistons, brake fluid and caliper body. This is, of course, heavily dependent on type of pad material.

The energy transferred during braking is directly related to the thermal resistance of the pad and disc surface. Assuming retardation is due entirely to friction in the brakes, we can express heat power generated per unit contact area at time t and r_{eff} :

$$q(r_{eff}, t) = F_{friction} \times r_{eff} (\omega_0 + at)$$

Directly connect this equation to known caliper parameters, the equation can be reformulated as a transient equation for heat power:

$$q(r_{eff}, t) = \left(\frac{P}{10} \times A_{piston} \right) \times \mu \times r_{eff} \left(\frac{\frac{rpm_0}{R_{gear}} \times \pi}{30} + \frac{\frac{rpm_0 - rpm}{R_{gear}} \times \pi \times t}{(t - t_0) \times 30} \right)$$

Where:

- A_{piston} caliper piston area
- P brake system pressure
- R_{gear} gearbox ratio
- rpm_0 motor rpm at the start of braking
- rpm motor rpm at the end of braking

This opens for plotting recorded vehicle sensor data into the equation, calculating heat power induced into the discs, stated by the number of set increments, from real world scenarios. As the vehicle will read a small amount of brake pressure, even during coasting and acceleration, the equation will give negative outputs of heat power, Effectively this will lead to a cooling effect on the brakes, with a factor much bigger than what the airflow would provide. Negative heat power values are therefore regarded as zero.

The heat conduction from simulations software models [COMSOL Multiphysics, 2012] in the disc and the pad can be described through the transient heat transfer equation:

$$\rho C_p \frac{\partial T}{\partial t} + \nabla \times (-k \nabla T) = Q - \rho C_p \times \nabla T$$

Where:

| | |
|--------|---|
| k | Thermal Conductivity ($W/(m K)$) |
| C_p | Specific heat capacity ($J/(kg K)$) |
| Q | heating power per unit volume (W/m^3) |
| ρ | density |

At the outer boundaries of the brake disc and pad, heat is produced according to equation 2.4 (and 2.5). Further we can describe the dissipating heat from the disc and pad surfaces to ambient air, with heat radiation and convective heat transfer:

$$q_{diss} = -h(T - T_{ref}) - \varepsilon \sigma (T^4 - T_{ref}^4)$$

Where:

| | |
|---------------|--|
| h | convective film coefficient (W/m^2K) |
| ε | material emissivity |
| σ | Stefan-Boltzmann constant ($5.67 \times 10^{-8} W/(m^2K^4)$) |
| $T - T_{ref}$ | temperature difference |

Furthermore, the convective film coefficient, h , can be expressed as a function of vehicle speed, v , with the following formula [*Chemical Engineering*, Vol. 1]:

$$h = \frac{0.037k}{D} \left(\frac{\rho D v}{\mu} \right)^{0.8} \left(\frac{C_p \mu}{k} \right)^{0.33}$$

Where:

| | |
|-------|------------------------------|
| D | disc diameter |
| μ | viscosity |
| C_p | specific heat capacity (air) |

The mentioned thermal equations are assuming uniform temperature distribution in all solids and fluids, with constant thermal properties.

2.3 Vehicle Dynamics

With designing a custom brake system, mass reduction is top priority along with functionality. Designing for mass reduction in suspension parts, comes with a lot of advantage, as we are effectively reducing unsprung mass. Explaining the effect of a reduction of unsprung mass in suspension systems, can be explained through the quarter-car model:

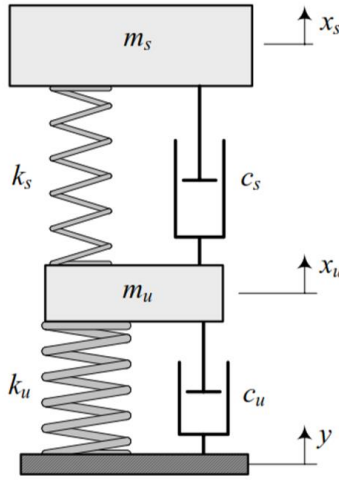


Figure 1 Quarter-car model [Jazar, 2017]

The quarter-car model illustrates two solid masses, acting as the sprung mass, m_s , and unsprung mass, m_u . These masses are equivalent to one wheel and the quarter mass of a vehicle. Furthermore, k_s and c_s represent the shock absorber, with a spring stiffness, k_s and a damper coefficient c_s . In addition, k_u and c_u are represent the spring-damper effect from the tire. The two masses are governed by these motion equations:

$$m_s \ddot{x}_s = -k_s(x_s - x_u) - c_s(\dot{x}_s - \dot{x}_u)$$
$$m_u \ddot{x}_u = k_s(x_s - x_u) + c_s(\dot{x}_s - \dot{x}_u) - k_u(x_u - y) - c_u(\dot{x}_u - \dot{y})$$

Translated into matrix form:

$$m\ddot{x} + c\dot{x} + kx = F$$

Where:

$$x = \begin{bmatrix} x_s \\ x_u \end{bmatrix}, \quad m = \begin{bmatrix} m_s & 0 \\ 0 & m_u \end{bmatrix}, \quad c = \begin{bmatrix} c_s & -c_s \\ -c_s & c_s + c_u \end{bmatrix}$$

$$k = \begin{bmatrix} k_s & -k_s \\ -k_s & k_s + k_u \end{bmatrix}, \quad F = \begin{bmatrix} 0 \\ k_u y + c_u \dot{y} \end{bmatrix}$$

The quarter-car model is a great tool in terms of tackling suspension vibrations. Complete suspension design requires several different simulating models. For the design of a brake system, the bicycle model is very useful.

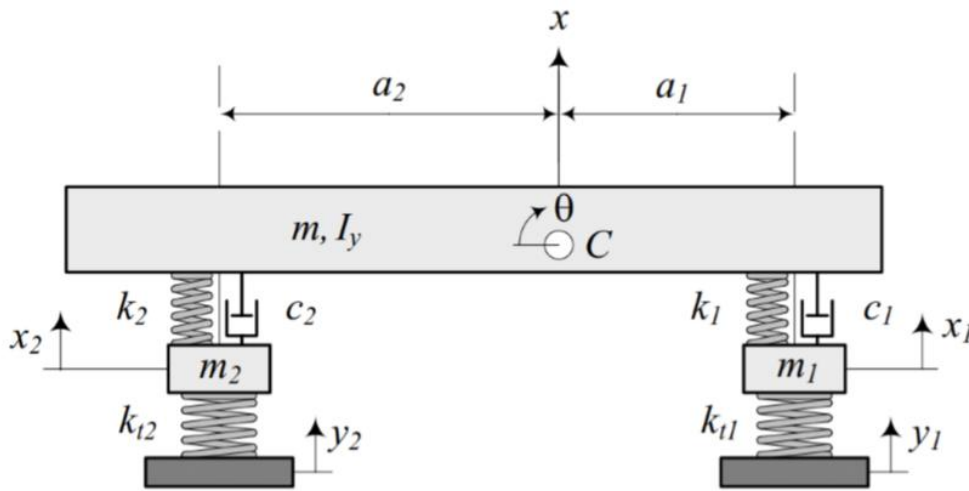


Figure 2 Bicycle-model [Jazar, 2017]

The bicycle model consists of three solid masses. The two smallest masses, m_1 and m_2 , are representing one front wheel and one rear wheel, where k_{t1} and k_{t2} is the spring stiffness of the tire. Tire dampening is ignored. The body of the vehicle has mass, m , with a lateral mass moment of inertia, I_y . Both m and I_y are values of a rigid bar, which are exactly half of the total vehicle. c_1 and c_2 represent the dampening coefficient and k_1 and k_2 represent the stiffness of the shock absorber.

The bicycle model can be formulated in matrix form as:

$$m\ddot{x} + c\dot{x} + kx = \mathbf{F}$$

Where:

$$x = \begin{bmatrix} x \\ \theta \\ x_1 \\ x_2 \end{bmatrix}, \quad m = \begin{bmatrix} m & 0 & 0 & 0 \\ 0 & I_z & 0 & 0 \\ 0 & 0 & m_1 & 0 \\ 0 & 0 & 0 & m_2 \end{bmatrix}, \quad \mathbf{F} = \begin{bmatrix} 0 \\ 0 \\ y_1 k_{t1} \\ y_2 k_{t2} \end{bmatrix}$$

$$c = \begin{bmatrix} c_1 + c_2 & a_2 c_2 - a_1 c_1 & -c_1 & -c_2 \\ a_2 c_2 - a_1 c_1 & c_1 a_1^2 + c_2 a_2^2 & a_1 c_1 & -a_2 c_2 \\ -c_1 & a_1 c_1 & c_1 & 0 \\ -c_2 & -a_2 c_2 & 0 & c_2 \end{bmatrix}$$

$$k = \begin{bmatrix} k_1 + k_2 & a_2 k_2 - a_1 k_1 & -k_1 & -k_2 \\ a_2 k_2 - a_1 k_1 & k_1 a_1^2 + k_2 a_2^2 & a_1 k_1 & -a_2 k_2 \\ -k_1 & a_1 k_1 & k_1 & 0 \\ -k_2 & -a_2 k_2 & 0 & k_2 \end{bmatrix}$$

From this model, estimations about pitch, given the dynamic load distribution between front and rear axle, can be calculated with regards to front and rear braking load.

It can be seen from both models, that an increase in mass will increase the force, \mathbf{F} . To compensate for a higher force. If the spring stiffness and dampening coefficient is unchanged, this will result in a longer wheel travel, consequently increasing damper frequency. Increase in damper frequency will result in less tire-ground adhesion. One might think, increasing damper coefficient and spring stiffness will fix the problem, but now the total forces have increased, meaning components need to be heavier to account for that force adding more mass.

2.4 Topology Optimization

Topology optimization is a method for optimizing structural load paths. It is a numerical method, distributing material in each design domain to maximize global stiffness of a component under certain constraints and objectives. For the brake caliper, the constraints are the design space, load case and bolt connections. Topology optimization can be formulated with the following equation [Skoglund, 2019]:

$$TO = \begin{cases} \text{minimize } f(x, y) \text{ with respect to } x \text{ and } y \\ \text{subject to } \begin{cases} \text{behavioral constraints on } y \\ \text{design constraints on } x \\ \text{equilibrium constraint} \end{cases} \end{cases}$$

Where:

$f(x, y)$ objective function, solving for max- or minimization

Behavioural constraints on y represent the structures response, for example, displacement, strain-energy, weight, volume, etc. *Design constraint on x* is a vector describing the design and load paths, for instance material properties. Finally, the *equilibrium constraint* is defined as:

$$\mathbf{K}(x)u = \mathbf{F}(x)$$

For the brake caliper design the most suitable objective function is to minimize strain energy. Strain energy for isotropic materials, is defined as a linear area of tensile stress-strain curve multiplied by the volume for the specimen. The strain energy objective equation favours low stress and structural compliance. Strain energy, U , is formulated as:

$$U = \frac{1}{2}V\sigma\varepsilon$$

2.5 Additive Manufacturing

Additive manufacturing, more commonly known as 3D-printing, is a process where three dimensional objects are built by layered material, like plastic, metal, concrete or biological materials. Common AM technology uses 3D models from CAD software and digitally slice the model into thin layers. This can then be replicated as a three-dimensional object in the printer.

For metals, the most common way of additive production is selective laser melting (SLM). SLM is a rapid prototyping manufacturing technique, that use powerful lasers to fuse metal powder. SLM manufacturing use a variety of alloys, from carbon steel to space grade aluminium and titanium. With selective laser melting, thin layers of fine metal powder are distributed on a metal printer plate, inside a closed space filled with inert gases such as nitrogen or argon and small amounts of oxygen. When metal powder is settled and evenly distributed, a two-dimensional slice of the model is fused together by the laser, followed by the same repeating process. The laser energy is high enough to weld the particles together to form a solid. This process allows for incredible design freedom.

To ensure functionality and manufacturability of AM parts, some guidelines are necessary. For titanium parts, model features with more than 20-30° degrees of overhang relative to the printer plate, need support structures to get good fusing of powder. Aluminium will need the same support structure from 45° overhang, consequently needing more support structure on average. As printing often happens at room tempered conditions, with high local temperatures from the laser, support structures can be a tool to lead heat away from the melt and reduce risk of print failure. Surfaces interfering with other components, such as bearings, bolts, and tolerance fitting parts, require post machining, as AM manufacturing generally give bad surface finishes compared to traditional subtractive machining.

2.6 Materials

Weight and stiffness are two defining design criteria a brake caliper design. Material stiffness can be defined as deformation resistance in elastic objects. For an object with loads translating into tension and compression, the stiffness, k , can be express as:

$$k = \frac{AE}{L}$$

Where:

- E modulus of elasticity (Young's Modulus)
- A cross-sectional area
- L component length

From the equation, stiffness conditions are based on both material properties (E) and object geometry (A and L). Stiffness can be linked to weight/mass with the equation:

$$k_{mat} = \frac{E}{\rho}$$

Where:

- ρ material density
- k_{mat} specific material stiffness

Suitable materials for caliper design are investigated. Differences in specific stiffness are small and indicates that geometric obtainable stiffness and thermal properties are the differentiating factors for both material choice and manufacturing method.

Table 1 Material properties and its specific stiffness

| | Density [g/cm ³] | E-modulus [GPa] | Specific Stiffness |
|------------------|------------------------------|-----------------|--------------------|
| AlSi10Mg | 2.670 | 70 | 26.22 |
| Steel MS1 | 8.100 | 140 | 17.28 |
| Ti6Al4V | 4.410 | 110 | 24.94 |

From the table, AlSi10Mg is the best of the available alternatives in terms of specific stiffness. Further investigation of AlSi10Mg and Ti6Al4V is therefore needed.

Thermal properties of the materials are crucial for consistent brake performance, as high operating temperatures lower Young's modulus and increase strain. The aluminium alloy has a higher thermal conductivity than the titanium alloy. Research on scientific papers done on these materials, show a profound difference between them in terms of mechanical properties with applied thermal load.

Table 2 Mechanical properties of AM-SLM AlSi10Mg specimens at various temperatures according to [*High-temperature mechanical properties of AlSi10Mg...*, 2017]:

| Test temperature, °C | Elastic modulus (E), GPa | Yield stress (YS), MPa | Ultimate tensile stress (UTS), MPa | Elongation at fracture (ϵ_f), % | Reduction of area, % |
|----------------------|--------------------------|------------------------|------------------------------------|--|----------------------|
| 25 | 77.6 | 204 | 358 | 7.2 | 8.7 |
| 50 | 75.5 | 198 | 341 | 8.5 | 9.2 |
| 100 | 72.8 | 181 | 286 | 10.0 | 11.1 |
| 150 | ^a | 182 | 241 | 14.7 | 15.8 |
| 200 | ^a | 158 | 189 | 16.4 | 18.7 |
| 250 | ^a | 132 | 149 | 30.9 | 50.3 |
| 300 | ^a | 70 | 73 | 41.4 | 67.4 |
| 350 | ^a | 30 | 33 | 53.8 | 81.9 |
| 400 | ^a | 12 | 14 | 57.4 | 96.0 |

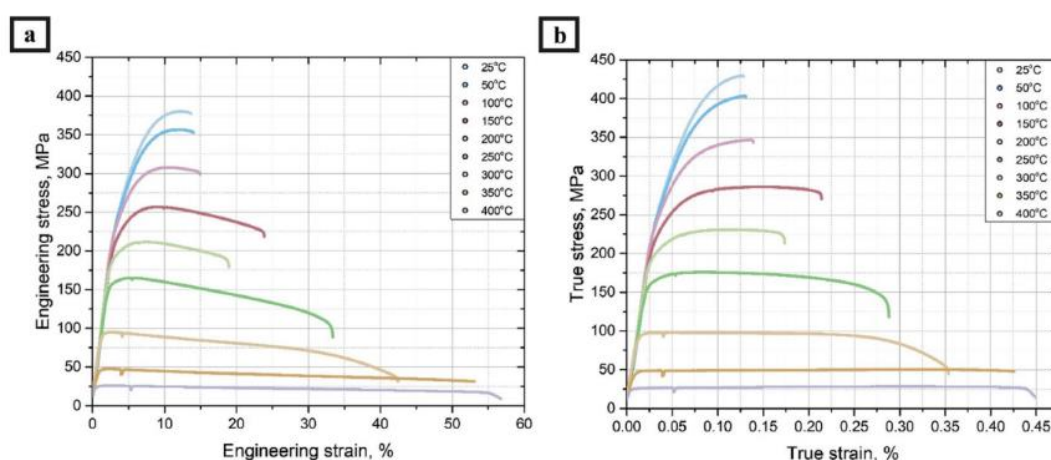


Figure 3 Tensile curves of SLM AlSi10Mg at various temperatures; (a) engineering stress-strain curves and (b) true stress-strain curves

Interpreting **Table 1** and **Fig. 3**, the aluminium alloy is prone to fast deterioration of mechanical properties, when subjected to thermal loads above 100 Degrees Celsius.

Table 3 Mechanical properties of AM-SLM Ti6Al4V specimens at various temperatures according to [Titanium Powder Metallurgy, 2015]

| Temperature (°C) | Thermal expansion, α_e ($1^\circ\text{C}^{-1}\times 10^{-6}$) | Elastic modulus, E (GPa) | Poisson's ratio, μ | Yield strength, σ_y (GPa) | Shear modulus, τ (MPa) |
|---------------------|--|---|---------------------------|---|--|
| 25 | 2.9 | 114.7 | 0.32 | 11.47 | 887 |
| 200 | 3.4 | 105.3 | 0.33 | 10.53 | 847 |
| 500 | 4.4 | 89 | 0.34 | 8.9 | 778 |
| 800 | 5.7 | 75 | 0.35 | 7.5 | 334 |
| 995 | 6.9 | 72.3 | 0.38 | 72.3 | 38 |
| 1200 | 7.65 | 64.6 | 0.39 | 64.6 | 27 |
| 1400 | 7.9 | 56.8 | 0.40 | 56.8 | 17 |
| 1650 | 8.6 | 45.4 | 0.41 | 45.4 | 3.8 |
| 1900 | 9 | 0 | 0.5 | 0 | 0.38 |

Interpreting **Table 3**, the titanium alloy is considerably more robust against thermal loads, showing little decrease in mechanical properties, even at 200 Degrees Celsius.

Chapter 3

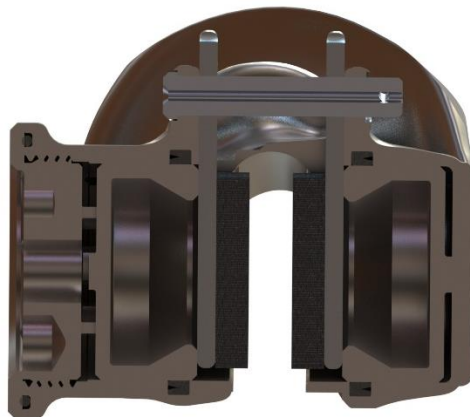
3 Brake Caliper and Load Case

This chapter will be an introduction to the brake caliper, and a description of the load case.

3.1 The Brake Caliper

The brake caliper is an assembly, housing brake pads and pistons. In commercial automotive and bicycle industry, the brake caliper is often made of aluminium, steel, or different plastics.

The most commonly known, are floating and fixed calipers. A floating caliper moves in relation to the disc. When pressure is applied, a single piston is pushing the pad on one side of the disc, meanwhile the caliper body pulls the opposite brake pad towards the disc. Floating calipers are susceptible to stiction, from environmental factors such as dirt and oxidation. Unlike a floating caliper, a fixed caliper does not move in relation to the disc. This means that the caliper is more susceptible for imperfections or out of tolerance discs. As the caliper requires intricate brake fluid routing and plural pistons, the fixed caliper is often more expensive, but have more balanced inner and outer pad wear, giving less tapering of the pads and more predictable braking.



Split view of the inhouse developed dual piston caliper

3.2 Load Case Analysis and KERS

The kinetic energy recovery system, or *KERS*, is the main system for braking. The mechanical brake system is there to accompany *KERS*, as this is not available before the accumulator is slightly discharged due to overcharging. As this system has limited torque output at the motors top rpm (shown in the **Fig. 4**), the vehicle top speed is the dimensioning load.

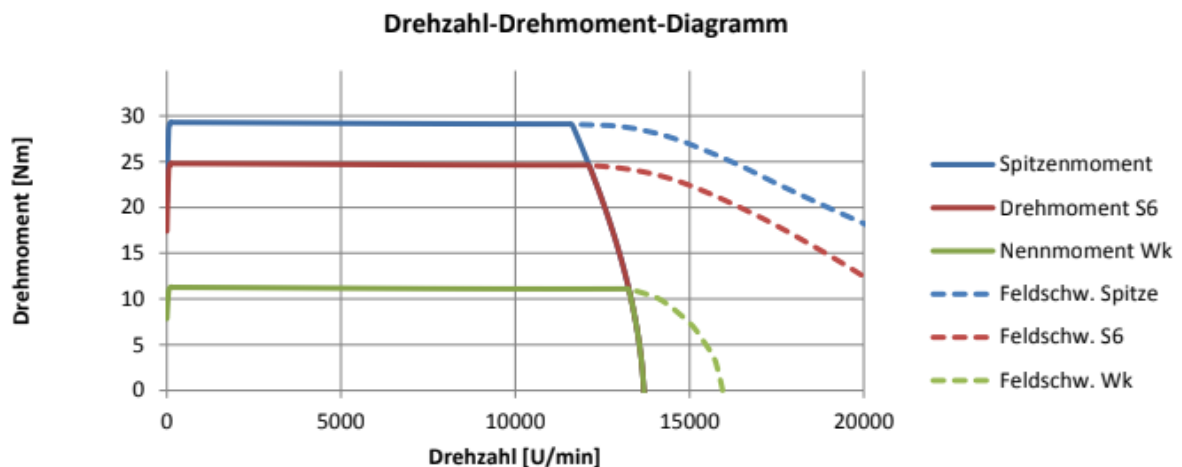


Figure 4 Available motor torque at given RPM [Appendix C]

Good engineering practice is for the tires to be the limiting factor of the car. Even if it is motor design or brake design, this should always be the case, as the car should be able to exploit every bit of the tire's performance when driving. The load case will therefore be based on the limits of the tire.

The chosen tires for 2020 are the *Continental C19*. Marius Nordrik, in charge of suspension points and overall dynamics of the car, made a dynamic tire model in MATLAB from Continentals data, with the use of the Pacejka M5.2 tire model. The general expression of the Pacejka tire formula:

$$y = D \times \sin\{C \times \arctan[Bx - E(Bx - \arctan(Bx))]\}$$

Where:

| | |
|-------------------|---|
| B, C, D and E | Fitting constants, dependent on application |
| y | force or moment resulting from a slip parameter |
| x | slip parameter |

A lap time simulation was made, implementing the tire model, vehicle load transfer, aerodynamic- and motor representations; too calculate the load case for the brake system. As the system requires more mass to accommodate a brake system with too high available braking force, the simulations were done to find the minimum braking force that does not compromise lap times (see **Fig. 5**, **Fig. 6**, and **Fig. 7**)

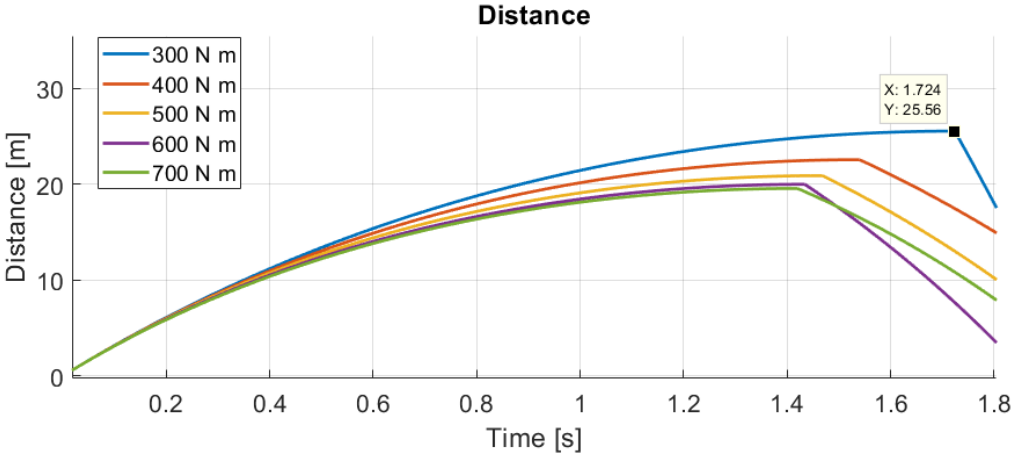


Figure 5 Sweeps of available torque was conducted with v equal to top speed

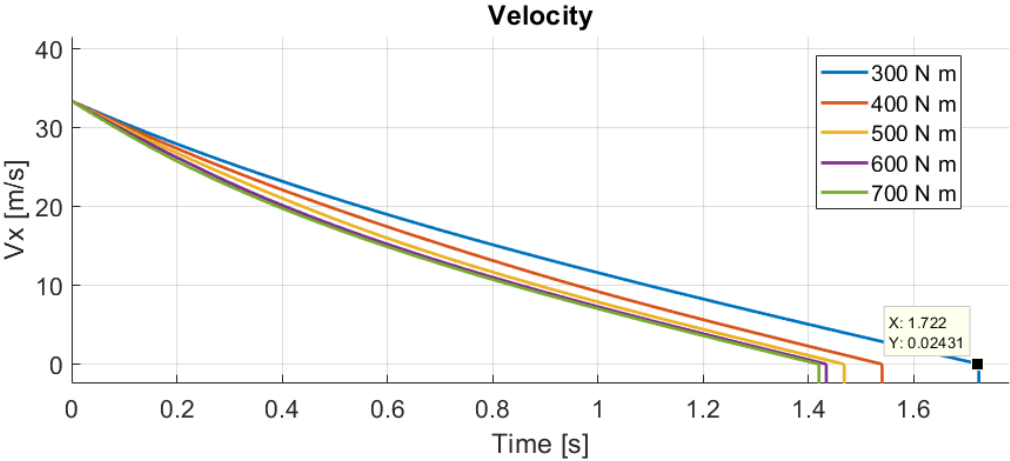


Figure 6 Lap times, showing braking from 120 km/h to 0 km/h for different

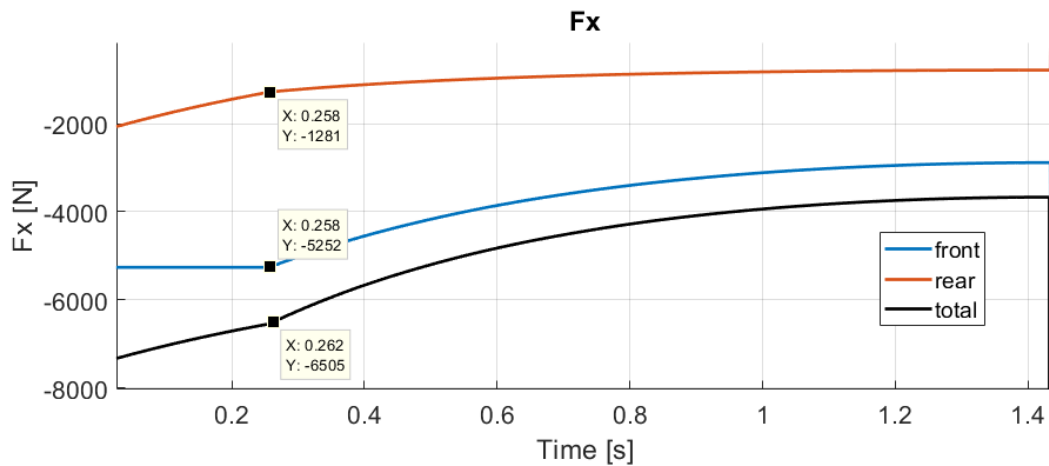


Figure 7 Distribution of longitudinal forces, require 0.8 brake balance to the

A lot of uncertainties revolve around the actual temperatures transferring from the discs (from measured live data) and to the calipers. Estimates are calculated and compared to live data recorded from two consecutive autocross runs at Formula Student Austria (2019), without *KERS* assistance, **Fig. 8.** show the temperature development:

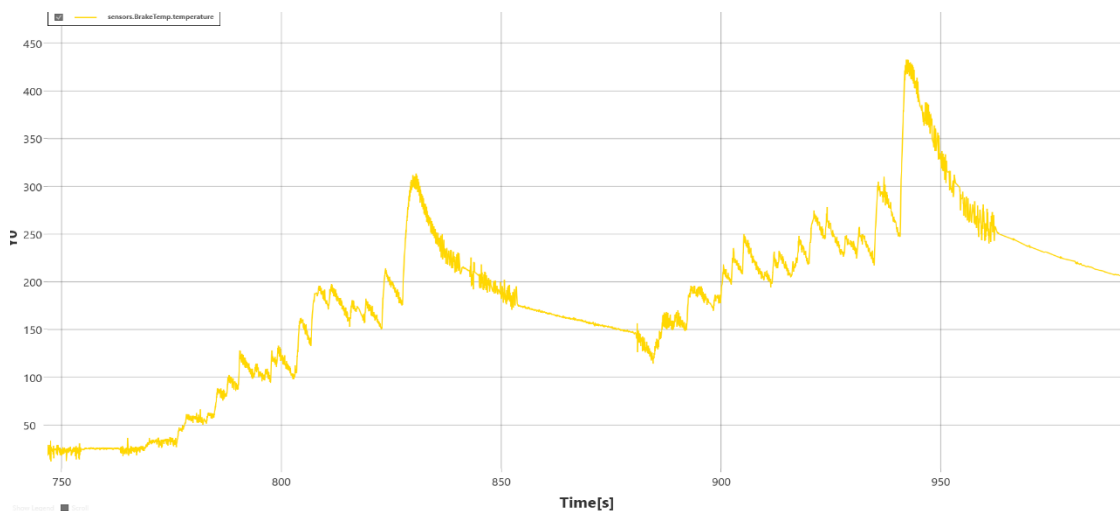


Figure 8 Temperature development of Revolve NTNU steel brake disc Revolve

Chapter 4

4 Brake Caliper Design

This chapter will describe the design philosophy and methodology used for designing the brake calipers. This is followed by a description of tasks done in Abaqus/CAE and TOSCA and a look at the completed designs.

4.1 Learning from previous calipers in Revolve

Revolve is developing in a fast pace, taking engineering work to a new level every year. Learning from what was working and what did not, is important in engineering.

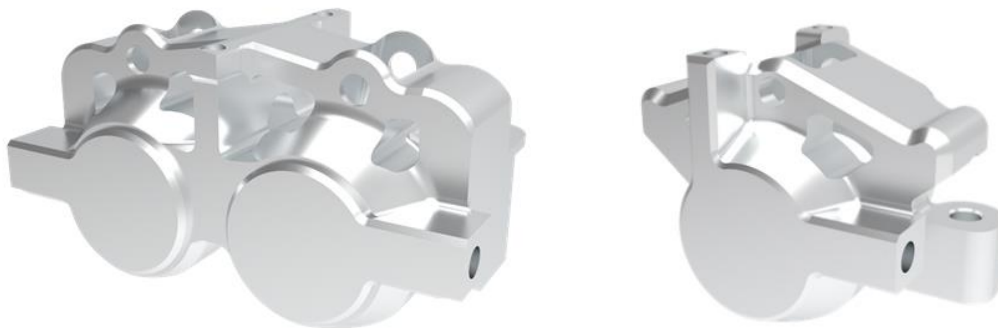


Figure 9 CNC machined calipers from 2018 – 330 grams front, 180 grams rear

The calipers from in **Fig. 9** were the first inhouse developed calipers and an experimental project in 2018. The goal was to reduce weight from the off-shelf ISR calipers used in previous years. This project started what would later become important research for future brake system design in Revolve. The topology optimized caliper was nearly 60 percent of the weight of the ISR's.



Figure 10 3D-printed front brake caliper from 2019 – 311 grams – and the Formula ROR rear caliper - 115 grams

The 2019 caliper (see Fig. 10) was also an experimental project, developed as a side project by a combination of members from 2019, in parallel with their own systems. The design of the front caliper, was super light, topology optimized and printed in space grade aluminium. This also one of the stiffest calipers, with a displacement of 0.33 mm magnitude displacement. Rear calipers were the off-shelf Formula ROR caliper, initially developed for downhill bicycles, mounted opposite to each other right and left wheel, due to it not being symmetric.

Choosing materials, as previously investigated in chapter 2 (2.6 Materials), was dependent on what sponsors had available and material properties. Previous inhouse developed calipers in Revolve, manufactured in aluminium, experienced a few cases of “spongy” brake-feel (2019), piston stiction and leakage after continued driving (2018).

A number of reasons could cause this. Causes of stiction can be due to inadequate tolerancing, with regards to thermal expansion; dimensioning, leading to high displacements; and/or manufacturing inaccuracies. A lot need of features would need to be adjusted for CNC machinability, maybe sacrificing some of the intended function of the part.

In case of the 2019 caliper, spongy brake-feel is likely a result of heat transferring from the caliper and to the brake fluid. This causes small residues of water particles to vaporize into gas. Consequently, as gas is easier to compress than fluid, applied pressure to the brake pedal will feel spongy and unresponsive.

Learning from the two previous years and with advice from 2019 alumni, the decision was set on manufacturing in 3D printed titanium. This would fix some of the mentioned problems, with regards to better thermal properties, leading to less decrease in stiffness and expansion under thermal load and without sacrificing form over function.

4.1.1 Benchmark Caliper Testing

Testing of the off shelf calipers was conducted to determine what was acceptable displacement in the outboard with different pressures. Testing was done with a test jig as shown in **Fig. 11**:

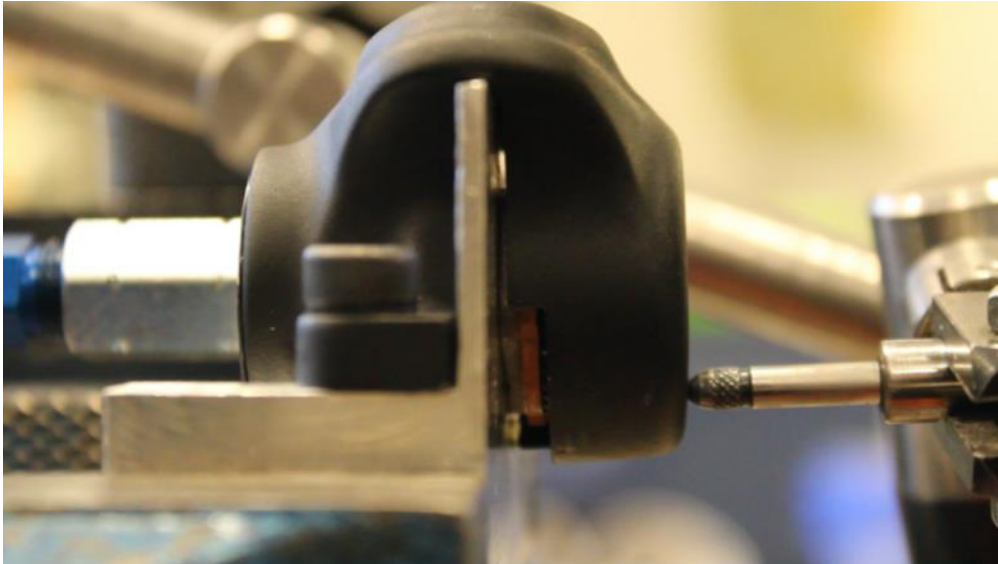


Figure 11 Pressure testing of the Formula ROR (Truls Skoglund)

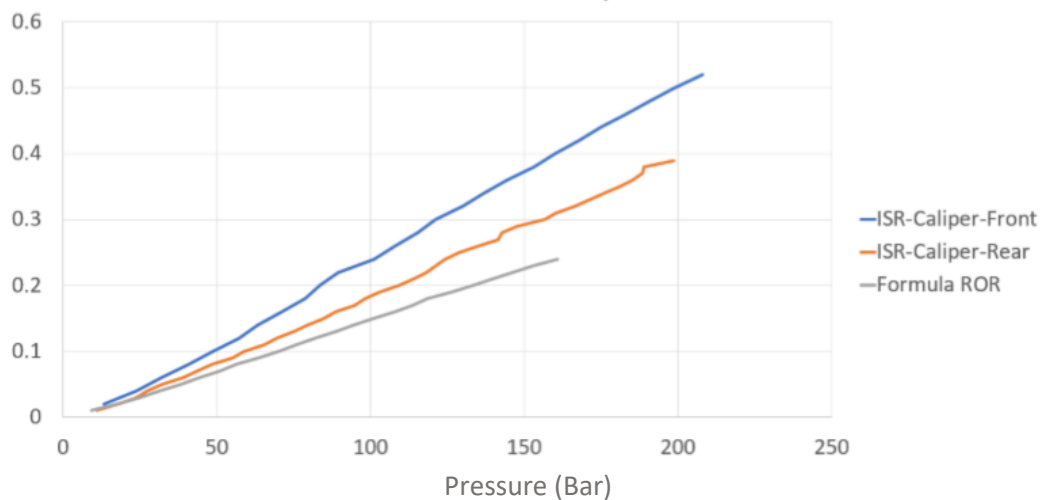


Figure 12 Deformation test results from off-shelf brake calipers

Seen in **Fig. 12**, deformation of the ISR front caliper is 0.5 mm at 200 bars. The the ISR rear caliper at the same pressure is deforming 0.4 mm. This is therefore be the maximum deformation allowed for the new in-house developed calipers. Formula ROR caliper should be used as a target for deformation, resulting in the stiffest caliper in this test.

4.2 Design Space

The design space of for the brake calipers are made with regards to the commercially available ISR brake calipers, rim interaction and upright interaction. This means that we both have backwards compatible calipers, allowing for interchangeability between inhouse-developed and commercial calipers on the car; and maximizing working area for the topology optimization algorithm from preliminary upright and rim design spaces. The design spaces for the front and rear calipers can be seen below in **Fig. 13**



Figure 13 Front and rear caliper design spaces seen in transparent material ISR calipers seen in grey.

4.3 Topology Optimization Setup

Topology optimization was done in TOSCA Structure as a plug-in in Abaqus/CAE (Dassault Systems) for the front caliper and ANSYS optimization for the rear calipers.

The two main optimization algorithms in TOSCA are *Sensitivity-based* and *Condition-based*. The sensitivity-based algorithm is the most flexible of the two, and is applicable for most problems, with objective functions and constraints being everything from stress to eigenfrequencies and modal loads. It is also less prone for mid-simulation failure. The condition-algorithm is more efficient but is limited to compliance related problems with only volume, weight, and strain objectives available in Abaqus/CAE (2017).

For the front caliper optimization, condition-based algorithm was used, as this gave the best results. The topology optimization was done without bolt connections, to reduce optimization time as it is less computationally expensive and allowed for more iterations with finer mesh.

Table 4 Front caliper topology optimization set-up

| | |
|--------------------------|--|
| Material | EOS Titanium Ti6Al4V |
| - E-modulus: | Anisotropic: XY 120 GPa, Z: 110 GPa |
| - Poisson Ratio: | 0.31 |
| - Density | 4.41 g/cm ³ |
| Element Type | Tetrahedral |
| - Mesh Size: | 1.0 |
| - No. Elements: | 2 334 921 (Front) and 1 981 349 (Rear) |
| Load Case: | Max brake, at 120 km/h / warm tires |
| Design Responses: | Condition-based algorithm |
| - Objective Function: | Min. Strain Energy |
| - Function Constraint: | Volume Frac. – Front 160 g and Rear 75 g |
| - Geometric Constraint: | Frozen piston and fluid channel surfaces |
| Design Cycles | 300 |

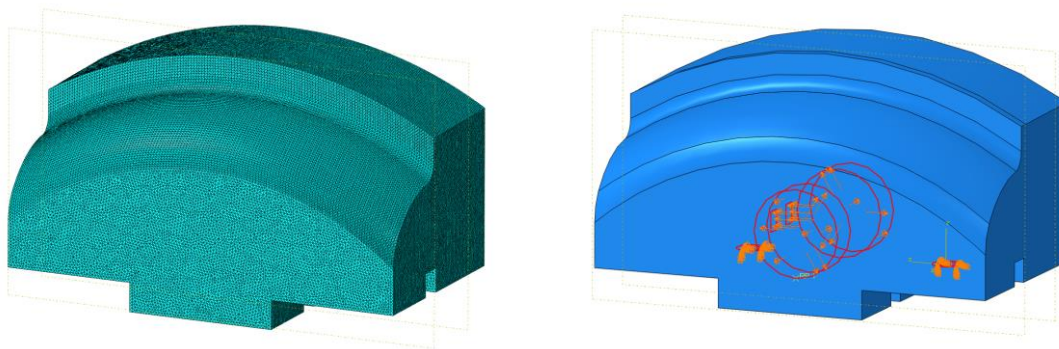


Figure 14 Front caliper design space mesh (left) and loads and constraints (right)

4.3.1 ANSYS Discovery Live

Being part of a sponsorship agreement, utilizing ANSYS for demonstrative purposes was done by Revolve NTNU. This meant trying out their latest software Discovery Live, a simulation and optimization software based on graphics card modelling rather than the more common computer processor modelling. This radically increased optimization speed, doing full live topology optimization with automatically generated CAD models in less than 1 hour. This allows for many iterations in a workday. Also, every model cycle can be seen in real-time as it optimizes.

What was interesting to investigate, was the difference between the TOSCA optimization and Discovery Live analysis. Revolve have a long history with FEM analysis in Abaqus/CAE, which made the perfect platform to validate the Discovery Live optimized model. As there is little literature about the accuracy of graphics optimization, this would be an interesting comparison and a potential opportunity for Revolve in the future.

The ANSYS software is limited to simple linear load cases, basic constraints, and sensitivity-based optimization algorithm. In terms of compliance directed optimization, the algorithm minimizes stress per volume and does not take displacement into consideration. This is not ideal for brake caliper optimization, but because of the linear load case, the brake caliper was the perfect candidate testing the software.

4.4 Topology Optimization Results

The front caliper topology optimization is modelled in TOSCA, while the rear caliper is optimized in ANSYS Discovery Live. Results can be seen in **Fig. 15**, **Fig. 16**, **Fig. 17**, and **Fig. 18** below.

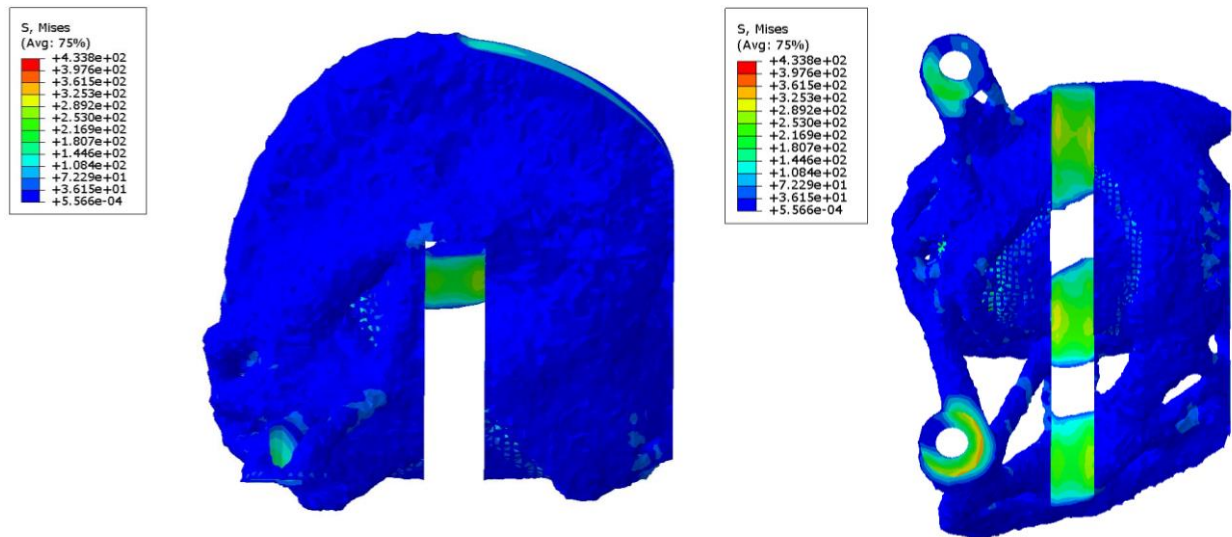


Figure 15 Front Caliper – Condition-based Algorithm (Strain-Volume) – Von Mises (Mpa)

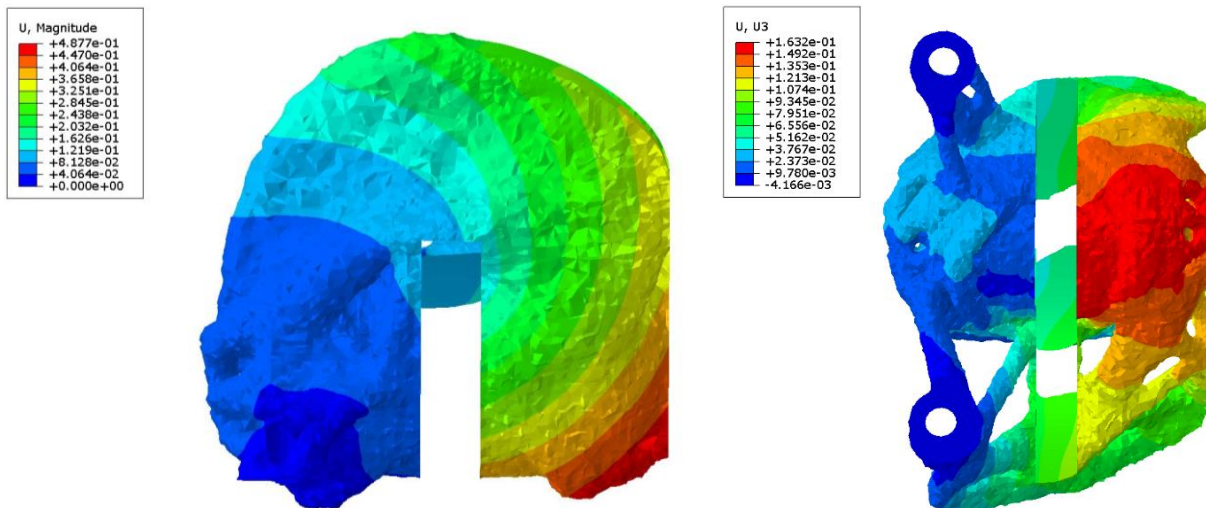


Figure 16 Front Caliper – Condition-based Algorithm (Strain-Volume) – Displacement (mm)

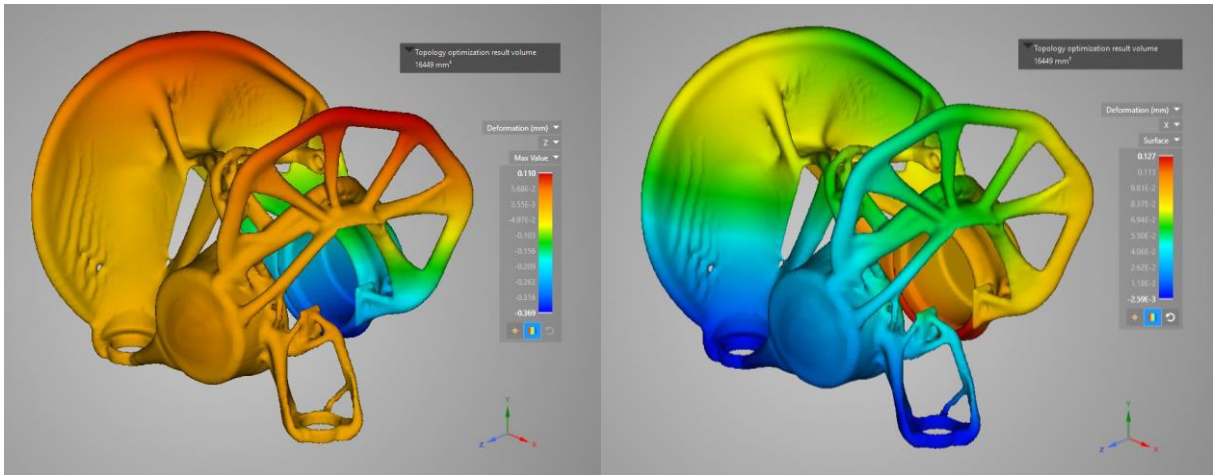


Figure 17 Rear caliper – Sensitivity-based Algorithm (Stress-Volume) – Displacement (mm) in Z- and X-direction

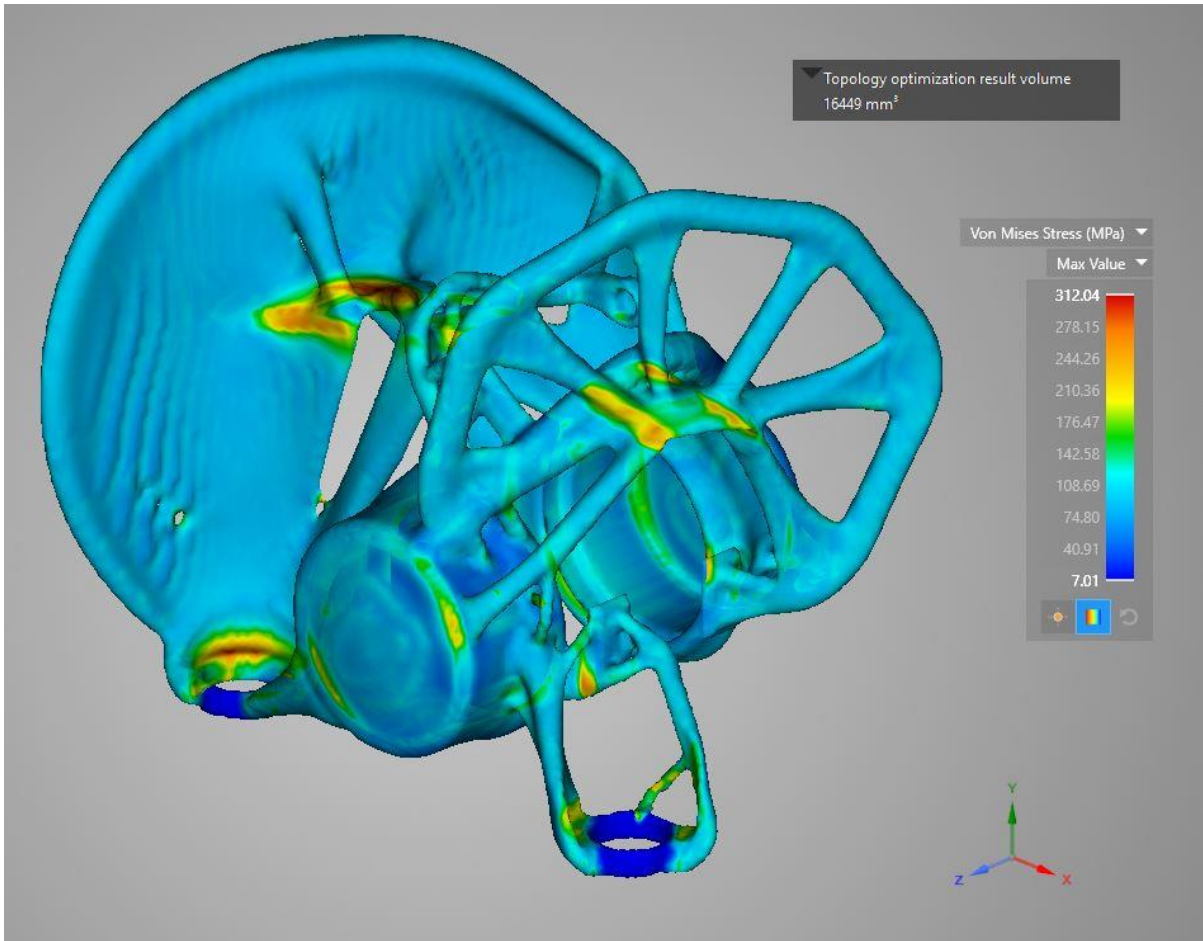


Figure 18 Rear Caliper – Sensitivity-based Algorithm (Stress-Volume) – Von Mises (Mpa)

4.5 Geometry Reconstruction

The models generated in TOSCA, are represented by the prechosen mesh. Consequently, raw topology models generally have a very rough surface when directly imported into SolidWorks. The model can be regenerated from importing point clouds or STL representation of the mesh model to be used as a guideline for modelling. The benefit is that all part features can be altered independently throughout the designing phase. All though this is beneficial for simpler geometries, it is very time consuming for complicated geometries. As this part will be additively manufactured, there are few geometric limitations leading to very complicated shapes.

In this case an alternative CAD regeneration method called *Power Surfacing* was used. Power surfacing smoothens the model from a solid imported STL-file from user's specification in a matter of minutes. This means that the detail CAD work can start much earlier, but it also means less commitment on every optimization geometry iteration. A disadvantage is that the imported geometry is allowed to deviate somewhat from the initial optimization result.

All planes are imported from the design space model, to ensure that all features are within the same spec. Interacting surfaces, such as piston chambers and seal surfaces are filled and cut-extruded to have full feature control. Fluid channels between chambers are generated in CAD, with a plane splitting the model at a 45° degree angle, located on the centre axis. The fluid channel is then drawn with spline lines, adjusted to be tangent to the part surface. This is done with consideration to support structure, as this part of the caliper is no reachable with any tools after print. A minimum angle limit for the fluid channel to be more than 45° in relation to the build plate, for this to be free of supporting material.

4.6 Final Caliper Design

Both front and rear caliper design is backwards compatible with the ISR 22-048 (front) and the ISR 22-049 (rear). The caliper housing can be seen in **Fig. 19** Below



Figure 19 Final AM- design of front (left) and rear caliper (right) housings

Complete assembly can be seen in **Fig. 4.6.2**. To be compatible both in terms of mounting and with the designed brake discs, the newly modelled calipers use brake pads supplied by ISR. The caliper is designed with standardized seals, supplied by Seal Engineering.

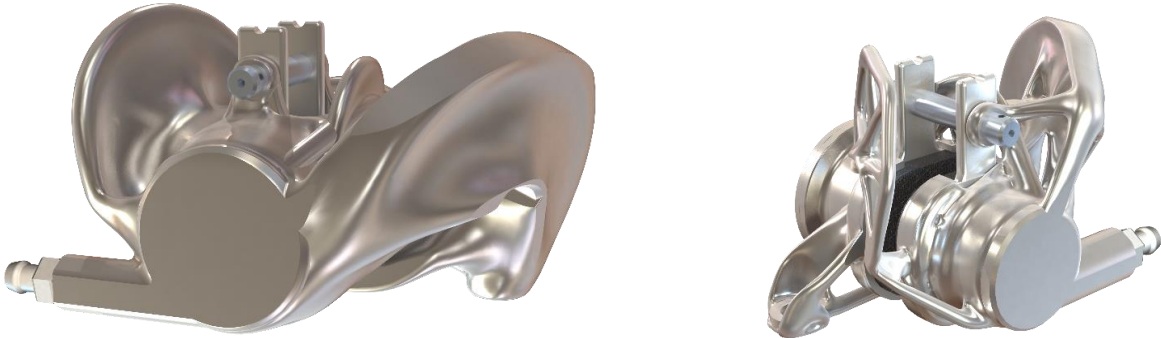


Figure 20 Front caliper (left) and rear caliper (right) assemblies

Table 5 Weight Comparison

| Assembly | Weight (g) |
|---------------------------------|------------|
| ISR Front Caliper | 460 |
| ISR Rear Caliper | 290 |
| AM Front Caliper (2019) | 311 |
| Formula ROR Rear Caliper (2019) | 115 |
| AM Front Caliper (2020) | 286 |
| AM Rear Caliper (2020) | 122 |

The new AM titanium calipers are 50% lighter than the commercially available ISR calipers. Titanium calipers also supersede the front caliper by 25 grams, while the rear caliper is 7 grams heavier than the Formula ROR bicycle caliper. The advantage of the rear caliper for 2020 is that it is mirrored between right and left wheel. This results in an equal force path on the left and right uprights, theoretically leading to more even brake performance in the rear, but also a decrease in weight on the uprights.

4.7 FEM Validation

The FEM validation of the topology optimized models consist of two simulations. One with only the housing and one with an assembly (**Fig. 21**). The one with only housing was set up similarly to the optimization.

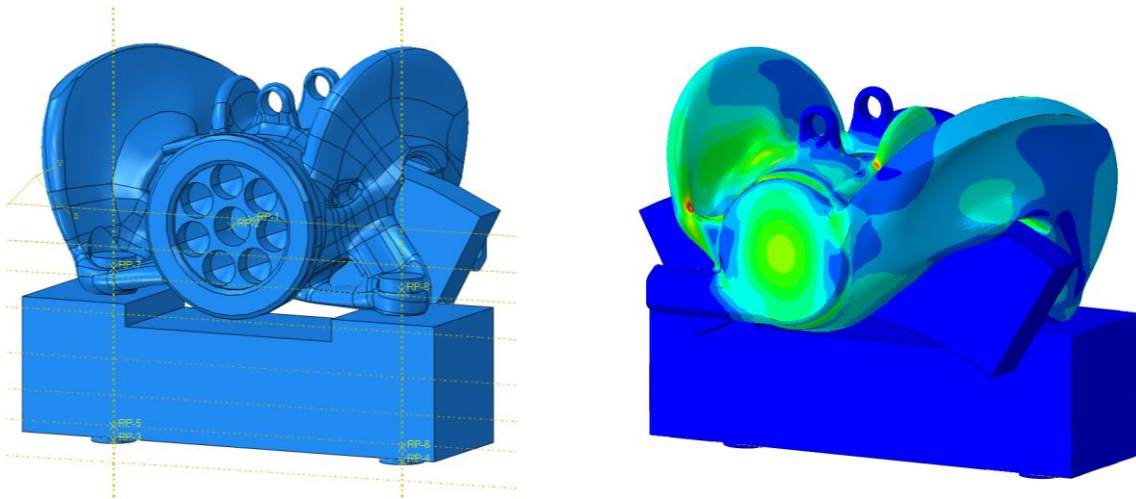


Figure 21 FEM validation – Assembly simulation

The assembly simulation consisted of a housing, two pistons, two bolts, a brake disc segment and a foundational element acting as the upright. Simulation steps are as follows:

- Pretension the two bolts with bolt loads (17 kN)
- Apply pressure to the inside of the housing and the pistons
- Apply a torque to the brake disc in normal driving direction

In this simulation, brake pads were neglected. To compensate for the brake pads thickness loss, the brake disc was made much thicker, leading to an equal piston travel with a case of very worn brake pads.

4.8 FEM Results

Front Caliper

The front caliper is way below the yield strength of titanium (Ti6Al4V), only reaching 400 MPa (disregarding high stress point nodes) and displacing 0.36 mm magnitude and 0.29 mm in the Z-direction.

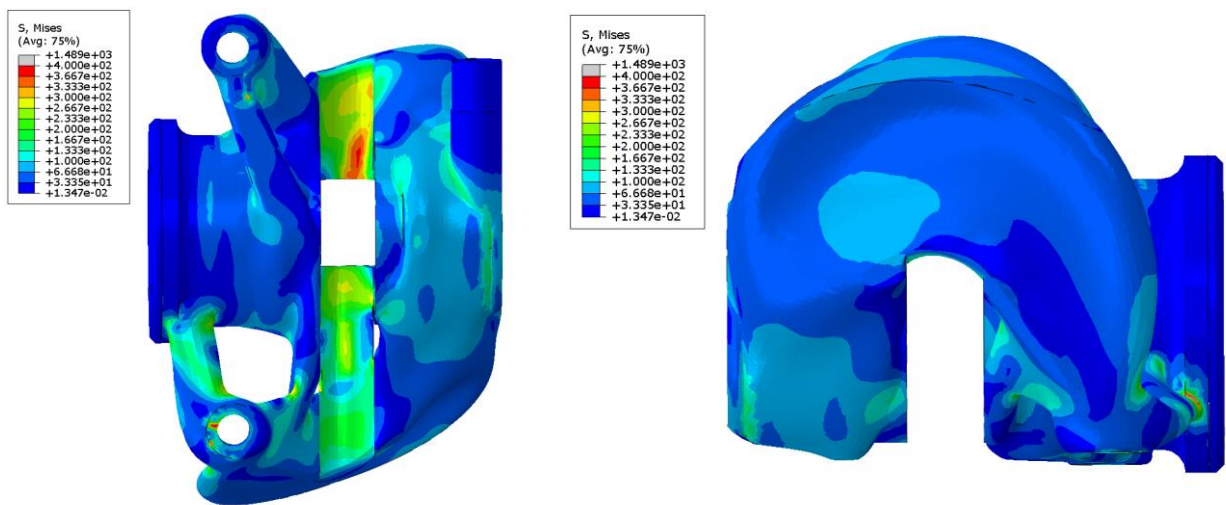


Figure 22 Front caliper housing – Von Mises (MPa) – Limit 400 MPa

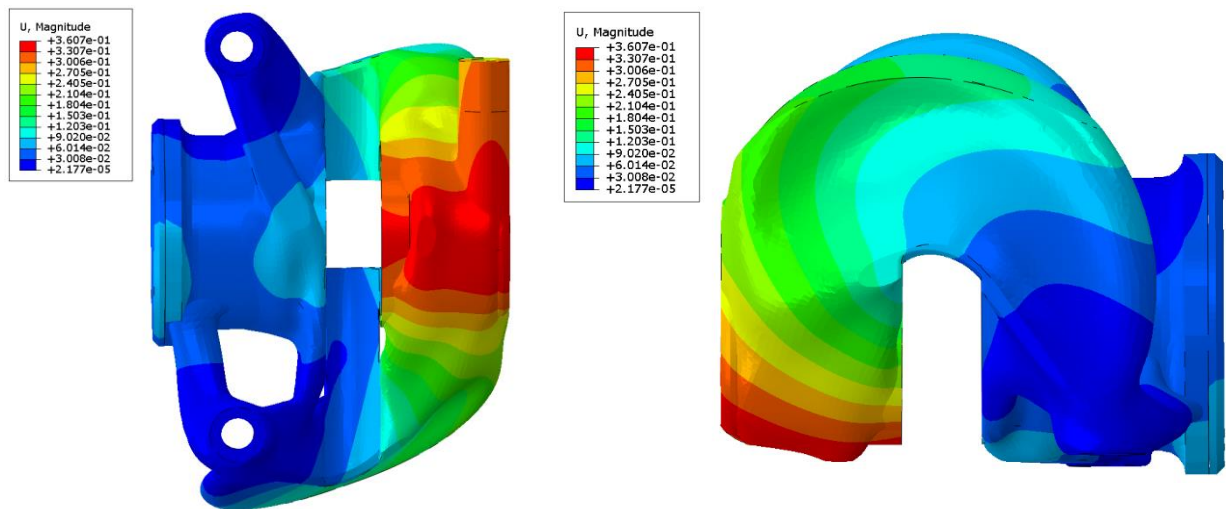


Figure 23 Front caliper housing – Magnitude displacement (mm)

Rear Caliper

The rear caliper is also far below the yield strength of titanium (Ti6Al4V), only reaching 426 MPa (including high stress point nodes) and displacing 0.42 mm magnitude and 0.31 mm in the Z-direction. Interesting point here is that the ANSYS Discovery Live model predicted a 0.36 mm displacement in the Z-direction.

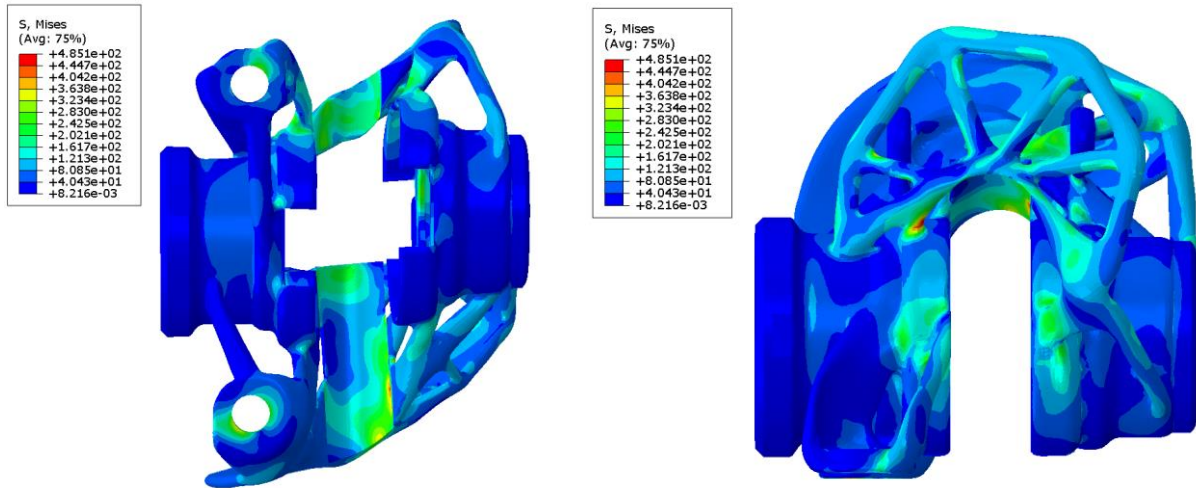


Figure 24 Rear caliper housing – Von Mises (MPa)

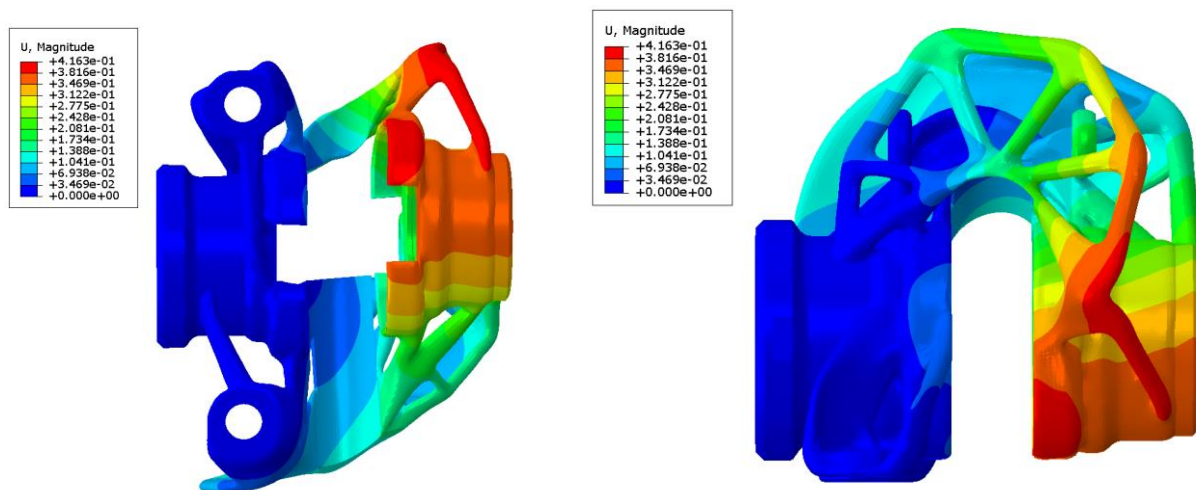


Figure 25 Rear caliper housing – Magnitude displacement (mm)

Chapter 5

5 Production

5.1 Manufacturing

The calipers are produced using additive selective laser melting manufacturing in titanium. Parts are printed with added support structure on angles smaller than 30° degrees from the build plate, avoiding support structure inside fluid channels. The caliper is printed with 5 mm extra material on all part interacting surfaces for machining purposes (see **Fig. 26**).

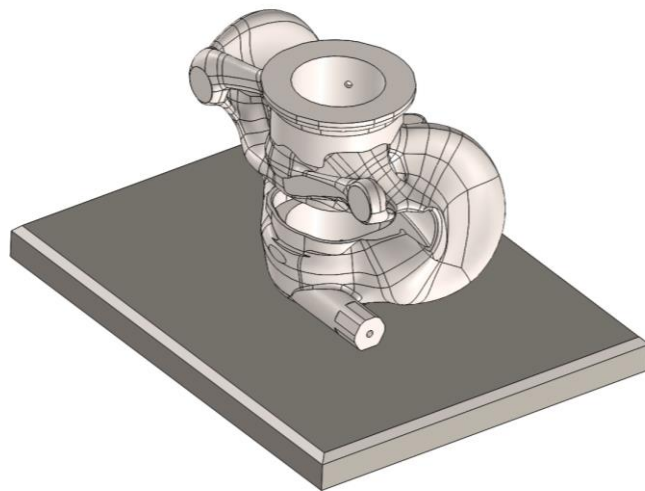


Figure 26 Front caliper, with extra material, on the build plate
(illustration without support structure)

To further maximize performance, careful considerations to factors influencing the production process is required. For a better chance of getting good tolerances, the printed specimens are sent through a 12-hour curing process before machining. As the part experiences uneven material heating in between the layers, tension will gradually build up in the part. The curing process will relieve the part from the internal stress that occurs during this process. This contributes to better overall material properties and lowering internal stresses. Consequently, improving tolerances, as machining can be done without risking it deforming when cutting it off the build plate. Not all factors are controllable during manufacturing, but appropriate actions were taken to minimize these.

5.2 Geometric Dimensioning and Tolerancing

The post machining process of the caliper housings and related parts requires careful planning of tolerances and description of each machining procedure. Interacting parts need careful tolerancing and geometric dimensioning, specifying allowable deviation in form, size, placement, surface, and shape. All of these variables control the overall reliability and performance of the part. Technical drawings (ISO TC213) can be seen in **Appendix F**.

Seal interacting surfaces are specified from Seal Engineering's *Tech Handbook 2019* [Appendix A]. Piston interacting surfaces, including the pistons are machined to a surface finish of 0.4 μm . The pistons are further being coated with a ceramic coating from Bodycote Sweden called *Tech 12* [Appendix A]. This is mainly to lower coefficient of friction to improve efficiency and decrease wear.

Piston fit tolerance in coherence with the housing tolerance, is carefully considered a long side the seal tolerances and thermal expansion rates derived from:

$$\Delta V = V_0 \times \alpha_V \times \Delta T$$

Where:

| | |
|------------|-------------------------------|
| ΔV | volume expansion difference |
| V_0 | volume at ambient temperature |
| α_V | thermal expansion coefficient |
| ΔT | temperature difference |

5.3 Assembly

Assembly of the parts are small and fit with tight tolerances. To ensure proper alignment and pressure on the joining parts, an assembly jig is used. This assembly jig (**Fig. 27**) was originally made for assembling Revolve NTNU's inhouse-designed PMSM electric motors, a process that require high accuracy and rigidity because of the high magnetic loads between the rotor and stator.



Figure 27 In-house designed assembly jig

Pressing tools are easily interchangeable and easy to manufacture. Also given that the press movement is done by hand through high tolerance trapezoidal threads, it is less likely to damage parts due to for instance galling or misalignment, compared to using a hydraulic press.

Assembly will be done by first inserting the S01-P single acting piston housing seal into its groove, heavily lubricated with either brake fluid or assembly lubricant. Pistons will then be press fitted into the housing, also heavily lubricated. Finally, the O-ring and end cap is installed with the correct torque spec and the bleed screw and hydraulic connectors are tightened to company provided specification at 200 bars.

5.4 Mechanical Testing

The planned mechanical testing of the new 2020 calipers are currently cancelled, from the recent development of the COVID-19 virus.

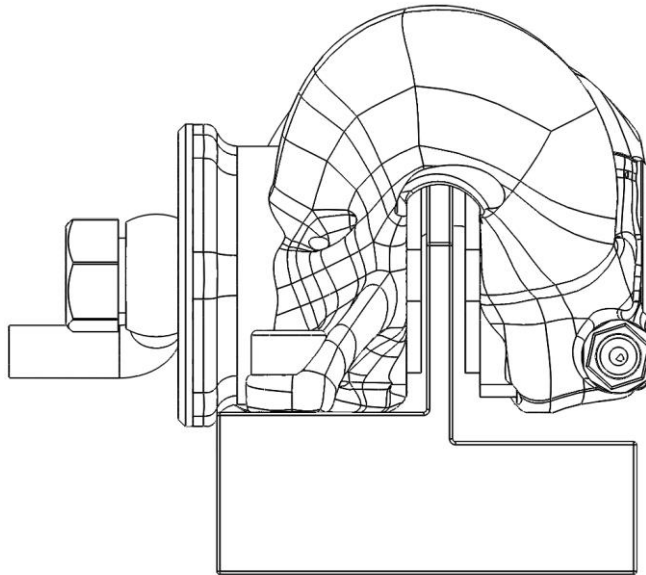


Figure 28 Caliper test jig

A test plan was developed, where the calipers are loaded at different pressures at increments of 10 bar. At each pressure increment, displacement will be measured with a dial gauge (See test jig on **Fig. 28**).

Furthermore, a brake fluid pressure-temperature sensor [Appendix A] was planned embedded into the hydraulic system of the brakes. That would mean live measurements of the brake fluid temperature during driving, alongside the infrared sensor implemented in 2019 for disc temperature measurement. Consequently, uncertainties from heat transfer estimations can be partially erased.

Chapter 6

6 Discussion

This thesis has dealt with the task of designing brake calipers for a Formula Student open-wheel race car. Description of the load case, both in mechanics and thermal load scenarios. Addressing the optimization model described in **4.3 Topology Optimization Setup**, many factors can and should be discussed.

Defining design domains, mesh, simplifying load scenarios, optimization setup and design objectives. When evaluating the optimized geometry, the optimization algorithm clearly used every outline of the design space. Being even more thorough when modelling the design space, even more area can be utilized, to further improve the resulting geometry of the algorithm. This could, in turn, lead to completely different geometries. Further, new caliper concepts that could be explored, such as single piston calipers opens up the opportunity to get a stiffer and smaller caliper. The three last years, caliper bolt patterns have consistently made it compatible with the ISR caliper. As the organization grow more confident in its ability, research could be done with different bolt patterns and how it affects stiffness and compliance. Further researching the answer for the question “*How much compliance and/or displacement can be allowed, to get the lightest possible part while maintaining high enough performance?*”, will have significant payoff for a plural number of systems on the car, and will slowly improve as the organization get more and more design documentation.

For 2021, Revolve NTNU will be exploring the in-wheel design concept for the first time. This opens up the possibility for using smaller and lighter 10-inch rim designs, including having motors integrated inside the rim. For caliper design, this will mean a significantly shrunk design space, leading to new design challenges. Investigating a longer stretching design space, similarly to formula 1 designs (see **Fig. 29**), with plural pistons or pistons only on one side of the caliper.



Figure 29 Brembo developed Formula 1 intended brake caliper.

The constant strive for simulation accuracy, is key to further development in engineering. For a system like the brake system, it is important to look beyond previous work and improve what have been done in previous years. Mechanical validation of FEM and optimization models are paramount. Models used in Revolve NTNU are always improving but are never accurate. One can argue that, although the components have been optimized, the finalized component is not. Further investigation into these subjects will in turn improve on these components. As more and more sensor data are available, a more accurate picture of the different component load scenarios is created and again open up for a wider selection of materials and design concepts.

With topology optimization, one can reduce design and concept span, compared to traditional design. With this being the third year of caliper development in Revolve NTNU, load cases and FEM models have been improving a little bit every year. The organization has had a huge set back with design validation in 2020, because of the COVID-19 virus as most new systems designs remain untested.

7 Conclusion

With the design and manufacturing overview, described in this thesis, it is clear that combining topology optimization and additive manufacturing increase performance within the same traditional design timeline. The results show that it is possible to directly produce optimized calipers designs based on topology optimization. Although not test verified, it is theoretically surpassing its commercial counterparts and proving to be a design approach providing high performance components. All though the design process is long, with multiple iterations from different design objectives and constraints, the results illustrate good capabilities of topology modelling. Tied with CNC machining, the final design perhaps is one of the more complex designs seen in Formula Student.

List of Figures

| | |
|---|----|
| Figure 1 Quarter-car model [Jazar, 2017] | 15 |
| Figure 2 Bicycle-model [Jazar, 2017] | 16 |
| Figure 3 Tensile curves of SLM AlSi10Mg at various temperatures; (a) engineering stress- strain curves and (b) true stress-strain curves | 20 |
| Figure 4 Available motor torque at given RPM [Appendix C] | 23 |
| Figure 5 Sweeps of available torque was conducted with v equal to top speed | 24 |
| Figure 6 Lap times, showing braking from 120 km/h to 0 km/h for different..... | 24 |
| Figure 7 Distribution of longitudinal forces, require 0.8 brake balance to the..... | 25 |
| Figure 8 Temperature development of Revolve NTNU steel brake disc Revolve | 25 |
| Figure 9 CNC machined calipers from 2018 – 330 grams front, 180 grams rear | 26 |
| Figure 10 3D-printed front brake caliper from 2019 – 311 grams – and the Formula ROR rear caliper - 115 grams | 27 |
| Figure 11 Pressure testing of the Formula ROR (Truls Skoglund) | 28 |
| Figure 12 Deformation test results from off-shelf brake calipers..... | 28 |
| Figure 13 Front and rear caliper design spaces seen in transparent material ISR calipers seen in grey. | 29 |
| Figure 14 Front caliper design space mesh (left) and loads and constraints (right) | 30 |
| Figure 15 Front Caliper – Condition-based Algorithm (Strain-Volume) – Von Mises (Mpa)..... | 32 |
| Figure 16 Front Caliper – Condition-based Algorithm (Strain-Volume) – Displacement (mm) | 32 |
| Figure 17 Rear caliper – Sensitivity-based Algorithm (Stress-Volume) – Displacement (mm) in Z- and X-direction..... | 33 |
| Figure 18 Rear Caliper – Sensitivity-based Algorithm (Stress-Volume) – Von Mises (Mpa)..... | 33 |
| Figure 19 Final AM- design of front (left) and rear caliper (right) housings | 34 |
| Figure 20 Front caliper (left) and rear caliper (right) assemblies | 35 |
| Figure 21 FEM validation – Assembly simulation..... | 36 |
| Figure 22 Front caliper housing – Von Mises (MPa) – Limit 400 MPa..... | 37 |
| Figure 23 Front caliper housing – Magnitude displacement (mm) | 37 |
| Figure 24 Rear caliper housing – Von Mises (MPa) | 38 |
| Figure 25 Rear caliper housing – Magnitude displacement (mm) | 38 |
| Figure 26 Front caliper, with extra material, on the build plate (illustration without support structure) | 39 |
| Figure 27 In-house designed assembly jig | 41 |
| Figure 28 Caliper test jig | 42 |
| Figure 29 Brembo developed Formula 1 intended brake caliper. | 44 |

List of Tables

| | |
|--|----|
| Table 1 Material properties and its specific stiffness..... | 19 |
| Table 2 Mechanical properties of AM-SLM AlSi10Mg specimens at various temperatures according to [High-temperature mechanical properties of AlSi10Mg..., 2017]:..... | 20 |
| Table 3 Mechanical properties of AM-SLM Ti6Al4V specimens at various temperatures according to [Titanium Powder Metallurgy, 2015]..... | 21 |
| Table 4 Front caliper topology optimization set-up..... | 30 |
| Table 5 Weight Comparison | 35 |

Bibliography

1. Aboulkhair, N. T., Maskery, I., Tuck, C., Ashcroft, I., Everitt. (2016) *Improving the fatigue behaviour of a selectively laser melted aluminium alloy: Influence of heat treatment and surface quality*, Materials & Design, Faculty of Engineering – University of Nottingham
2. Bendsøe, M.P. and Sigmund, O. (2003) *Topology Optimization Theory, Methods and Applications, 2nd ed.*, Springer-Verlag Berlin Heidelberg GmbH.
3. *BREMBO RECONFIRMS ITS COMMITMENT IN THE FORMULA 1 WORLD CHAMPIONSHIP WHICH, AS PER TRADITION, STARTS WITH AUSTRALIAN GP* (2018). Available: <https://www.brembo.com/en/company/news/brembo-formula-1-2018>, (Accessed: August 2019)
4. Chastand, V., Tezenas, A., Cadoret, Y., Quaegebeur P., Maia, W., Charkaluk, E. (2016) *Fatigue characterization of Titanium Ti-6Al-4V samples produced by Additive Manufacturing*, Villeneuve, France: Elsevier
5. Cai, C., Geng, H., Cui, Q., Wang, S., Zhang, Z. (2018) *Low cycle fatigue behaviour of AlSi10Mg (Cu) alloy at high temperature*, Beijing University of Aeronautics and Astronautics.
6. Chiumenti, M., Cervera, M., Lin, X., Lu X. (2018) *Finite Element Analysis and Experimental Validation of the Thermomechanical Behavior in Laser Solid Forming of Ti-6Al-4V*, University of Catalunya
7. Coulson, J.M. and Richardson J.F. (1999) *Chemical Engineering vol. 1*, Butterworth-Heinemann
8. Dassault Systèmes. (2017). *Abaqus Online Documentation*, Available: <http://50.16.225.63/v2016/index.html> (Accessed September 2019)
9. Heisler, H. (2002) *Advanced Vehicle Technology 2nd Edition*, London, UK, Butterworth-Heinemann
10. Guggiano M. (2014) *The Science of Vehicle Dynamics*, Italy, Pisa: Springer International Publishing.
11. Jazar, R.N. (2017) *Vehicle Dynamics, Theory and Application*, Melbourne, Australia: Springer International Publishing
12. Milliken, W.F., Milliken, D.S. (1997) *Race Car Vehicle Dynamics*, SAE International

-
13. Qian, M., and Froes, F.H. (2015) *Titanium Powder Metallurgy 1st ed*, School of Aerospace, Mechanical and Manufacturing Engineering, RMIT University, Melbourne
 14. Skoglund, T.M. (2019) *Dynamic and Process Dependent Integrity Investigations of a Topology Optimized Additive Manufactured AlSi10Mg Upright*, Norwegian University of science and technology.
 15. Society of Automotive Engineers International (2019), *2019-20 Formula SAE Rules*, www.fsaeonline.com (Accessed: August 2019).
 16. Uzan, N.E., Shneck, R., Yeheskel, O., Frage, N. (2018) *High-temperature mechanical properties of AlSi10Mg specimens fabricated by additive manufacturing using selective laser melting technologies (AM- SLM)*, University of Negev
 17. Uzan, N.E., Shneck, R., Yeheskel, O., Frage, N. (2017) *Fatigue of AlSi10Mg specimens fabricated by additive manufacturing selective laser melting (AM-SLM)*, University of Negev.
 18. Vasseljen, B. (2018) *CNC Manufactured Topology Optimized Brake Calipers*, Norwegian University of Science and Technology
 19. Low, I.M. (2006) *Ceramic Matrix Composites: Fiber Reinforced Ceramics and their Applications*, Curtin, Australia: Woodhead Publishing
 20. COMSOL Multiphysics (2012) *Heat Generation In a Disc Brake*, Available: <https://cdn.comsol.com/wordpress/2013/02/Step-by-step-guide-for-modeling-heat-generation-in-a-disc-brake.pdf> (Accessed September 2019)

Appendix

Appendix A: AlSi10Mg Material Properties

Appendix B: Ti64 Material Properties

Appendix C: Fischer Elektromotoren, Datasheet

Appendix D: Bodycote Tech 12, Datasheet

Appendix E: Seal Engineering, Datasheet

Appendix F: Technical Drawings

Appendix **A**

AlSi10Mg Material Properties

EOS Aluminium AlSi10Mg

EOS Aluminium AlSi10Mg is an aluminium alloy that has been specially optimised for processing on EOS M 400 systems.

This document contains information and data for building parts with EOS Aluminium AlSi10Mg powder (EOS part no. 9011-0024) in accordance with the following specifications:

- EOS M 400
- EOSPRINT v1.2 / EOSYSTEM v2.2.40
- AlSi10Mg 90µm FlexLine

Description

The alloy AlSi10Mg has good casting properties and is typically used for cast parts with thin walls and complex geometry. It is characterised by good strength and hardness, as well as high dynamic load bearing capacity, and it therefore also used for parts subjected to high loads. Parts made of EOS Aluminium AlSi10Mg are ideal for applications that require a combination of good thermal properties and low weight. They can be machined, wire eroded and electrical discharge machined, welded, micro-blasted, polished and coated.

Conventionally cast components made of this aluminium alloy are often heat-treated to improve the mechanical properties. For example using the T6 cycle, comprising solution annealing, quenching and artificial ageing. A special aspect of the laser sintering process is the extremely fast melting and re-solidification. Consequently, a structure with the related mechanical properties similar to the T6-treated cast parts results directly from the building process. For this reason, such heat treatments are not recommended for laser sintered parts, instead stress relief heat treatment for 2 hours at 300 °C is recommended. Due to the layering, the parts have anisotropic properties. These characteristics can be reduced or eliminated by suitable thermal post-treatment – see technical data for examples.

Material data sheet - FlexLine

Technical data

Powder properties

The chemical composition of the powder corresponds to the standard DIN EN 1706:2010

Material composition (wt%)

| Element | Min | Max |
|---------|------|------|
| Al | Rest | |
| Si | 9.0 | 11.0 |
| Fe | --- | 0.55 |
| Cu | --- | 0.05 |
| Mn | --- | 0.45 |
| Mg | 0.20 | 0.45 |
| Ni | --- | 0.05 |
| Zn | --- | 0.10 |
| Pb | --- | 0.05 |
| Sn | --- | 0.05 |
| Ti | --- | 0.15 |

Particle size

d90 [1] < 106 µm

[1] Laser diffraction in accordance with ISO 13320-1.

Material data sheet - FlexLine

General process data

| | |
|-----------------|--|
| Layer thickness | 90 µm |
| Volume rate [2] | 27.8 mm ³ /s (100.3 cm ³ /h) |

[2] The volume rate is a measure of the building speed during the exposure of the skin region. The total building speed is dependent on further factors such as the exposure parameters for contours, supports, Upskin and Downskin, the duration of the recoating, the home-in and LPM settings.

Physical and chemical properties of the parts

The chemical composition of the part corresponds to the standard DIN EN 1706:2010.

Material composition (wt%)

| Element | Min | Max |
|---------|------|------|
| Al | Rest | |
| Si | 9.0 | 11.0 |
| Fe | --- | 0.55 |
| Cu | --- | 0.05 |
| Mn | --- | 0.45 |
| Mg | 0.20 | 0.45 |
| Ni | --- | 0.05 |
| Zn | --- | 0.10 |
| Pb | --- | 0.05 |
| Sn | --- | 0.05 |
| Ti | --- | 0.15 |

| | |
|-----------------------------------|------------------------|
| Density [3] | 2.64 g/cm ³ |
| Roughness after microblasting [4] | Ra 11 µm; Rz 64 µm |

[3] Weighing in air and water in accordance with ISO 3369.

[4] Measurement of roughness as per ISO 4287. The values were determined on the vertical surface of a cube, as well as on the horizontal surface facing upward. Due to the layering, the surface structure is heavily dependent on the orientation of the surface, for instance a stepped effect is to be seen on inclined and round surfaces.

Material data sheet – FlexLine

Mechanical properties at room temperature [5, 6]

| | As built | After heat treatment [7] |
|-----------------------|----------|--------------------------|
| Tensile strength, Rm | 395 MPa | 290 MPa |
| Yield strength, Rp0.2 | 244 MPa | 165 MPa |
| Ultimate strain, A | 3.2 % | 7.3 % |

[5] The stated values are average values and were determined on samples with vertical and horizontal orientation.

[6] Mechanical strength tested as per EN ISO 6892-1:2009 B10, proportional bars, specimen diameter 5 mm, initial measured length 25 mm.

[7] Heat treatment: 300 °C / 2 h.

Abbreviations

Min. Minimum

Max. Maximum

Wt. Weight

The data apply for the combinations of EOS M400, EOSPRINT1.2 and parameter set AISi10Mg_90_FlexlineM400 specified on page 1 during processing as per parameter sheet M400_Parameter_sheet and the related applicable operating instructions. All measured values are average values and do not correspond to any specification. The part properties are determined using specified measuring processes as per defined test geometries and procedures. Further details on the test procedures employed by EOS are available on request. Deviations from the standard conditions can have an effect on the measured values.

The information reflects our knowledge and experience at the time of publication. As part of the continuous development and improvement processes at EOS, the information may be subject to change without notice. EOS does not provide any warranty for properties or suitability for specific applications, unless explicitly agreed. This statement also applies in relation to the protection of possible property rights as well as existing laws and regulations.

EOS[®], EOSINT[®] and DMLS[®] are registered trademarks of EOS GmbH.

© 2015 EOS GmbH – Electro Optical Systems. All rights reserved.

Appendix **B**

Ti64 Material Properties

EOS Titanium Ti64

EOS Titanium Ti64 is a titanium alloy powder which has been optimized especially for processing on EOSINT M systems.

This document provides information and data for parts built using EOS Titanium Ti64 powder (EOS art.-no. 9011-0014) on the following system specifications:

- EOSINT M 280 with PSW 3.6 and Original EOS Parameter Set Ti64_Speed 1.0
- EOS M 290 400W with EOSPRINT 1.0 and Original EOS Parameter Set Ti64_Performance 1.0 und Ti64_Speed 1.0

Description

Parts built in EOS Titanium Ti64 have a chemical composition corresponding to ISO 5832-3, ASTM F1472 and ASTM B348.

This well-known light alloy is characterized by having excellent mechanical properties and corrosion resistance combined with low specific weight and biocompatibility.

This material is ideal for many high-performance engineering applications, for example in aerospace and motor racing, and also for the production of biomedical implants (note: subject to fulfilment of statutory validation requirements where appropriate).

Due to the layerwise building method, the parts have a certain anisotropy, which can be reduced or removed by appropriate heat treatment - see Technical Data for examples.

Material data sheet

Technical data

General process and geometric data

| | |
|---|---|
| Typical achievable part accuracy [1], [8] | $\pm 50 \mu\text{m}$ |
| Min. wall thickness [2], [8] | approx. 0.3 – 0.4 mm approx. 0.012 – 0.016 inch |
| Surface roughness, as built [3], [8] | |
| Ti64 Performance (30 μm) | R_a 9 – 12 μm , R_z 40 – 80 μm R_a 0.36 – 0.47 x 10 ⁻³ inch, R_z 1.6 – 3.2 x 10 ⁻³ inch |
| Ti64 Speed (60 μm) | R_a 6 – 10 μm , R_z 35 – 40 μm R_a 0.23 – 0.39 x 10 ⁻³ inch, R_z 1.37 – 1.57 x 10 ⁻³ inch |
| Volume rate [4] | |
| Ti64 Performance (30 μm) | 5 mm ³ /s (18 cm ³ /h) 0.82 in ³ /h |
| Ti64 Speed (60 μm) | 9 mm ³ /s (32.4 cm ³ /h) 1.98 in ³ /h |

- [1] Based on users' experience of dimensional accuracy for typical geometries. Part accuracy is subject to appropriate data preparation and post-processing, in accordance with EOS training.
- [2] Mechanical stability is dependent on geometry (wall height etc.) and application
- [3] Due to the layerwise building, the surface structure depends strongly on the orientation of the surface, for example sloping and curved surfaces exhibit a stair-step effect. The values also depend on the measurement method used. The values quoted here given an indication of what can be expected for horizontal (up-facing) or vertical surfaces.
- [4] Volume rate is a measure of build speed during laser exposure. The total build speed depends on the average volume rate, the recoating time (related to the number of layers) and other factors such as DMLS-Start settings.

Material data sheet

Physical and chemical properties of parts

| | |
|----------------------|--|
| Material composition | Ti (balance) Al (5.5 – 6.75 wt.-%) V (3.5 – 4.5 wt.-%) O (< 2000 ppm) N (< 500 ppm) C (< 800 ppm) H (< 150 ppm) Fe (< 3000 ppm) |
| Relative density | approx. 100 % |
| Density | 4.41 g/cm ³ 0.159 lb/in ³ |

Material data sheet

Mechanical properties of parts [8]

| | As built | Heat treated [6] |
|--|---|--|
| Tensile strength [5] | | |
| - in horizontal direction (XY) | typ. 1290 ± 50 MPa typ. 187 ± 7 ksi | min. 930 MPa (134.8 ksi) typ. 1100 ± 40 MPa (160 ± 6 ksi) |
| - in vertical direction (Z) | typ. 1240 ± 50 MPa typ. 187 ± 7 ksi | min. 930 MPa (134.8 ksi) typ. 1100 ± 40 MPa (160 ± 6 ksi) |
| Yield strength (R_{p0.2}) [5] | | |
| - in horizontal direction (XY) | typ. 1140 ± 50 MPa typ. 165 ± 7 ksi | min. 860 MPa (124.7 ksi) typ. 1000 ± 50 MPa (145 ± 7 ksi) |
| - in vertical direction (Z) | typ. 1120 ± 80 MPa typ. 162 ± 12 ksi | min. 860 MPa (124.7 ksi) typ. 1000 ± 60 MPa (145 ± 9 ksi) |
| Elongation at break [5] | | |
| - in horizontal direction (XY) | typ. (7 ± 3) % | min. 10 % typ. (13.5 ± 2) % |
| - in vertical direction (Z) | typ. (10 ± 3) % | min. 10 % typ. (14.5 ± 2) % |
| Modulus of elasticity [5] | | |
| - in horizontal direction (XY) | typ. 110 ± 15 GPa typ. 16 ± 2 Msi | typ. 110 ± 15 GPa typ. 16 ± 2 Msi |
| - in vertical direction (Z) | typ. 110 ± 15 GPa typ. 16 ± 2 Msi | typ. 110 ± 15 GPa typ. 16 ± 2 Msi |
| Hardness [7] | typ. 320 ± 12 HV5 | |

[5] Tensile testing according to ISO 6892-1:2009 (B) Annex D, proportional test pieces, diameter of the neck area 5 mm (0.2 inch), original gauge length 25 mm (1 inch).

[6] Specimens were treated at 800 °C (1470 °F) for 4 hours in argon inert atmosphere. Mechanical properties are expressed as minimum values to indicate that mechanical properties exceed the minimum requirements of material specification standards. ASTM F1472-08. By fulfilling these minimum values, also the specifications of standards ASTM B348-09 and ISO 5832-3:2000 are met.

[7] Vickers hardness measurement (HV) according to EN ISO 6507-1 on polished surface. Note that measured hardness can vary significantly depending on how the specimen has been prepared.

[8] Hint: these properties were determined for Ti64_Performance 1.0 on an EOSINT M 280-400W and EOSINT M 290-400W. Test parts from Ti64_Speed 1.0 were determined on machine types EOSINT M 280-400W and correspond with data from an EOS M 290-400W.

Material data sheet

Thermal properties of parts

| | |
|---|----------------------------------|
| Maximum long-term operating temperature | approx. 350 °C approx. 660 °F |
|---|----------------------------------|

Abbreviations

| | |
|---------|---------------|
| typ. | typical |
| min. | minimum |
| wt. | weight |
| approx. | approximately |

Notes

The data are valid for the combinations of powder material, machine and parameter sets referred to on page 1, when used in accordance with the relevant Operating Instructions (including Installation Requirements and Maintenance) and Parameter Sheet. Part properties are measured using defined test procedures. Further details of the test procedures used by EOS are available on request.

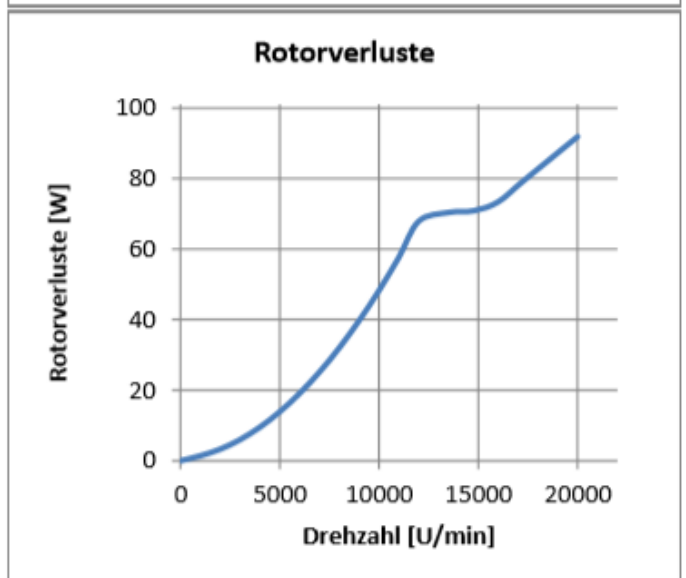
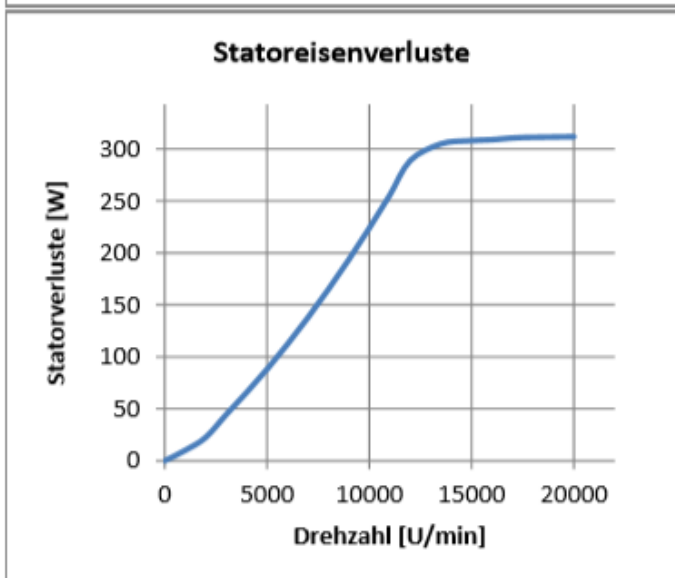
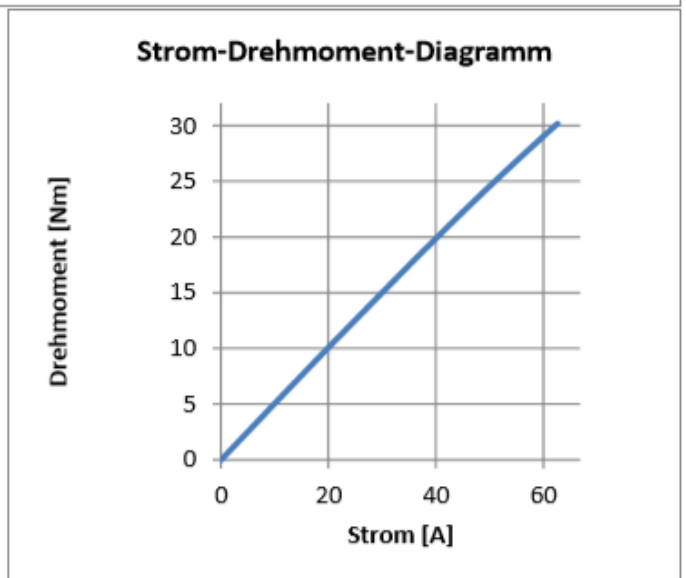
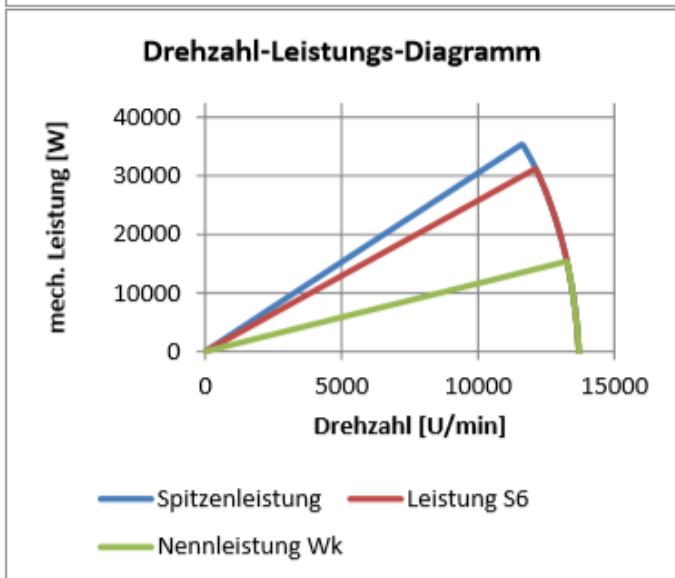
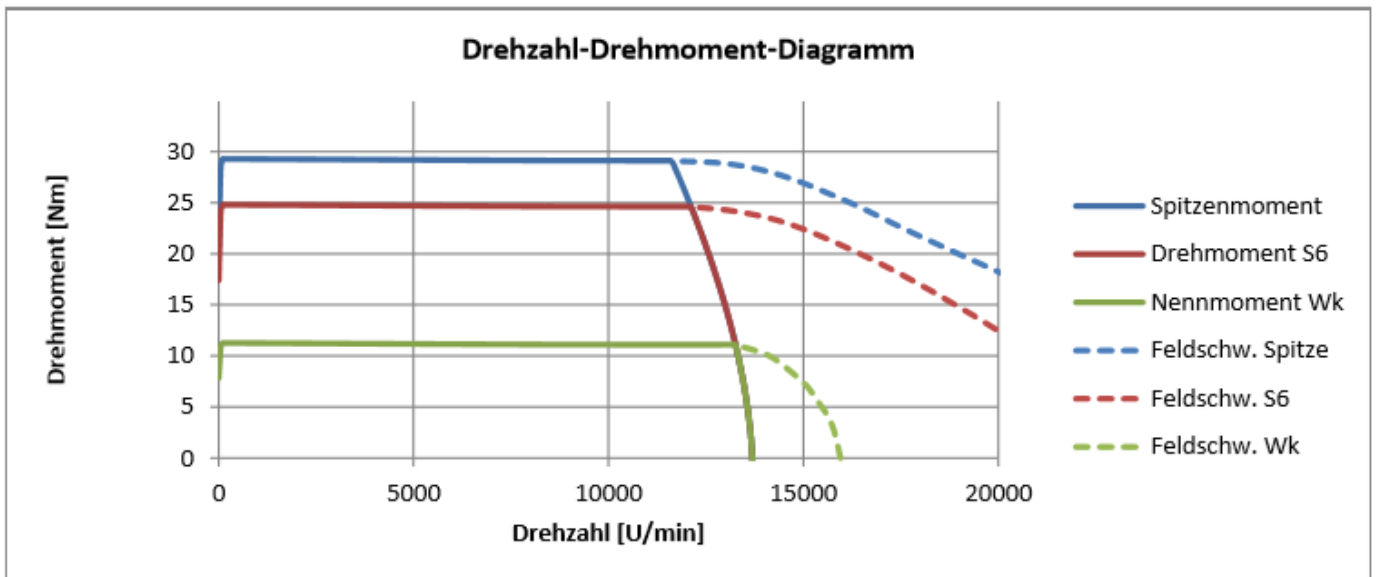
The data correspond to our knowledge and experience at the time of publication. They do not on their own provide a sufficient basis for designing parts. Neither do they provide any agreement or guarantee about the specific properties of a part or the suitability of a part for a specific application. The producer or the purchaser of a part is responsible for checking the properties and the suitability of a part for a particular application. This also applies regarding any rights of protection as well as laws and regulations. The data are subject to change without notice as part of EOS' continuous development and improvement processes.

EOS[®], EOSINT[®] and DMLS[®] are registered trademarks of EOS GmbH.

© 2014 EOS GmbH – Electro Optical Systems. All rights reserved.

Appendix **C**

Fischer Elektromotoren, Datasheet



Appendix **D**

Bodycote Tech 12, Datasheet

Process Datasheet

TECH 12

For increased wear resistance, corrosion resistance, and anti-galling with little dimensional change

TECH 12 bonds ceramic with a metal surface by chemically reacting with other oxides produced on that surface.

TECH 12 etches and penetrates into surface grain boundaries. The strength of the ceramic oxide-to-metal bond is exceptionally strong, preventing flaking or particle pull-out even at 0.5% beyond the yield point of the metal.

THICKNESS OF ONLY 0.0002 INCHES

TECH 12 does not typically require pre-machining. It has a thickness of less than 0.0002 inches (5 microns) and a penetration into the substrate of less than 0.0005 inches (12 microns).

HARDNESS

TECH 12 has a Vickers hardness of 2850. Comparatively, hard chrome plate is 850 to 1000 Vickers and tungsten carbide is 1900 Vickers. This hard ceramic, well bonded to the substrate, provides a wear surface that can withstand wear by most materials. The sealed surface prevents crevice-corrosion, especially in o-ring grooves of down-hole oil service tools, by preventing corrosives from reaching the metal substrate.

LOW FRICTION

TECH 12 produces a surface that has a coefficient of friction of 0.11 - 0.13, depending on the substrate texture and the contact material. The combination of low friction and high particle hardness can increase resistance to galling by threads, especially when the same material is used for both thread components.

PROPERTIES

- Has thickness of less than 0.0002"
- Is chemically bonded into substrate
- Will not change dimensions
- Is low friction
- Offers sliding wear resistance

TECHNICAL DATA

| | |
|-------------------------|--|
| Max Hardness | Up to 2850 Vickers |
| Bond Mechanisim | Chemical |
| Bond Strength | Over 10,000 PSI |
| Thickness | 0.0002 Inches |
| Coefficient of friction | 0.22 - 0.28 Against fiber, 0.1 - 0.13 Against metal |

Appendix **E**

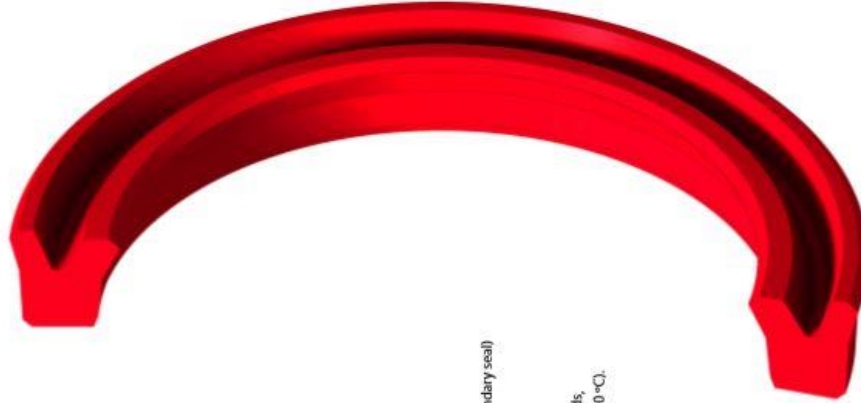
Seal Engineering, Datasheet

Rod seals – housing recommendations

S01-P is our standard u-cup rod seal. This profile can be produced in different polyurethanes, with HPU being the most versatile and widely used.



S01-P profile



S01-P in HPU

S01-P

S01-P has the following advantages:

- Excellent static and dynamic sealing
- Good back-pumping ability
- High wear resistance/operational reliability
- Good chemical resistance
- Can be used as an individual seal or as secondary seal within sealing systems
- Small cross sections possible

Technical data:

- Material:** HPU
Pressure: Up to 400 bar
Speed: Up to 0.5 m/s (1.5 m/s possible if used as secondary seal)
Temperature: -20 °C to 110 °C
Media: Mineral based hydraulic oils, HFA and HFB fluids, biologically degradable oils and water (up to 90 °C).

Table 6, Wiper A26-F. Dimensions recommended for standard housing.

| ød | øD | øD ₁ | L | R ₁ (max) | R ₂ (max) | O-ring (2x) |
|-----------|---------|-----------------|------|----------------------|----------------------|-------------|
| 20 – 50 | ød+7.6 | ød+1.0 | 4.2 | 0.4 | 0.2 | BS 0xx/1.78 |
| 40 – 80 | ød+8.8 | ød+1.5 | 6.3 | 1.2 | 0.2 | BS 1xx/2.62 |
| 70 – 165 | ød+12.2 | ød+2.0 | 8.1 | 2.0 | 0.2 | BS 2xx/3.53 |
| 140 – 525 | ød+16.5 | ød+2.0 | 11.5 | 2.0 | 0.2 | BS 3xx/5.33 |
| 400 – 650 | ød+24.0 | ød+2.5 | 15.5 | 2.0 | 0.2 | BS 4xx/6.99 |
| > 650 | ød+27.3 | ød+2.5 | 18.0 | 2.0 | 0.2 | 8.4 |



A26-F

Table 7, Wiper A27-F. Dimensions recommended for standard housing.

| ød | øD | øD ₁ | L | R ₁ (max) | R ₂ (max) | O-ring |
|-----------|---------|-----------------|------|----------------------|----------------------|-------------|
| 6 – 70 | ød+4.8 | ød+1.5 | 3.7 | 0.4 | 0.2 | BS 0xx/1.78 |
| 12 – 155 | ød+6.8 | ød+1.5 | 5.0 | 0.7 | 0.2 | BS 1xx/2.62 |
| 45 – 325 | ød+8.8 | ød+1.5 | 6.0 | 1.0 | 0.2 | BS 2xx/3.53 |
| 145 – 540 | ød+12.2 | ød+2.0 | 8.4 | 1.5 | 0.2 | BS 3xx/5.33 |
| 265 – 650 | ød+16.0 | ød+2.0 | 11.0 | 1.5 | 0.2 | BS 4xx/6.99 |
| > 400 | ød+20.0 | ød+2.5 | 14.0 | 2.0 | 0.2 | 8.4 |



A27-F

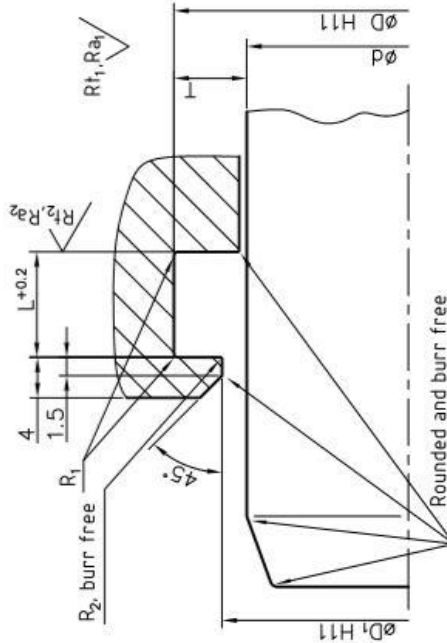
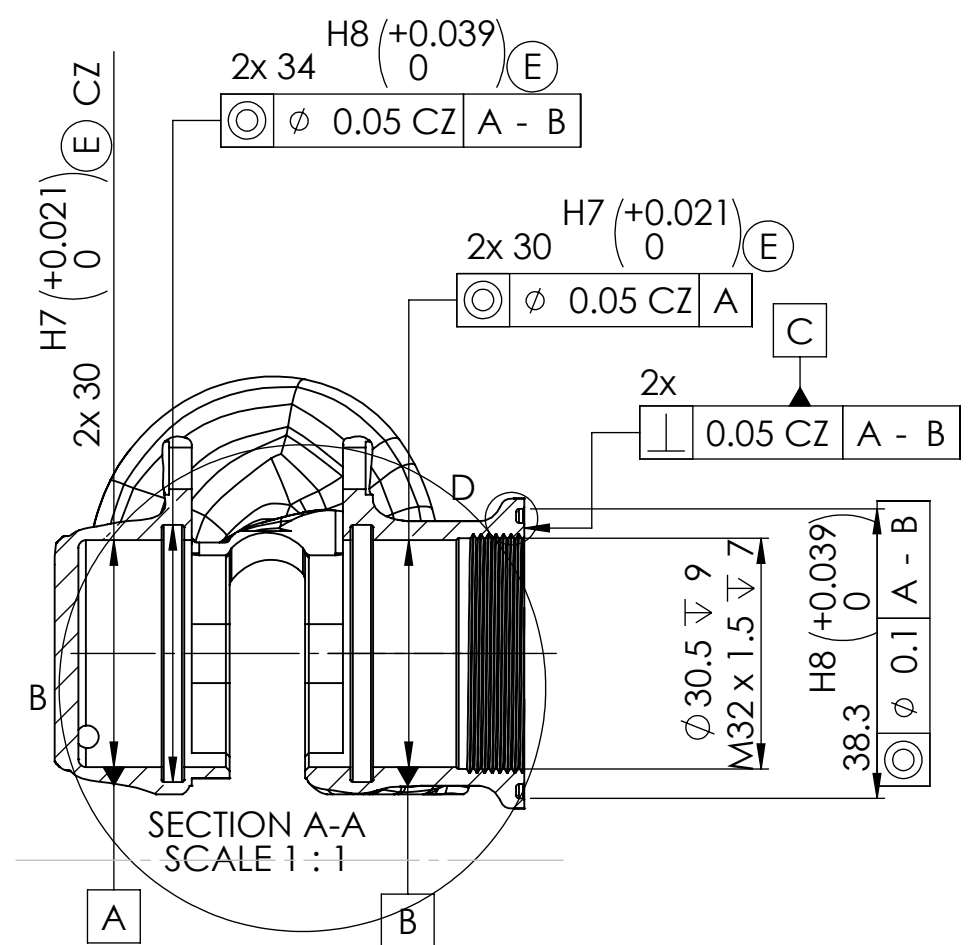
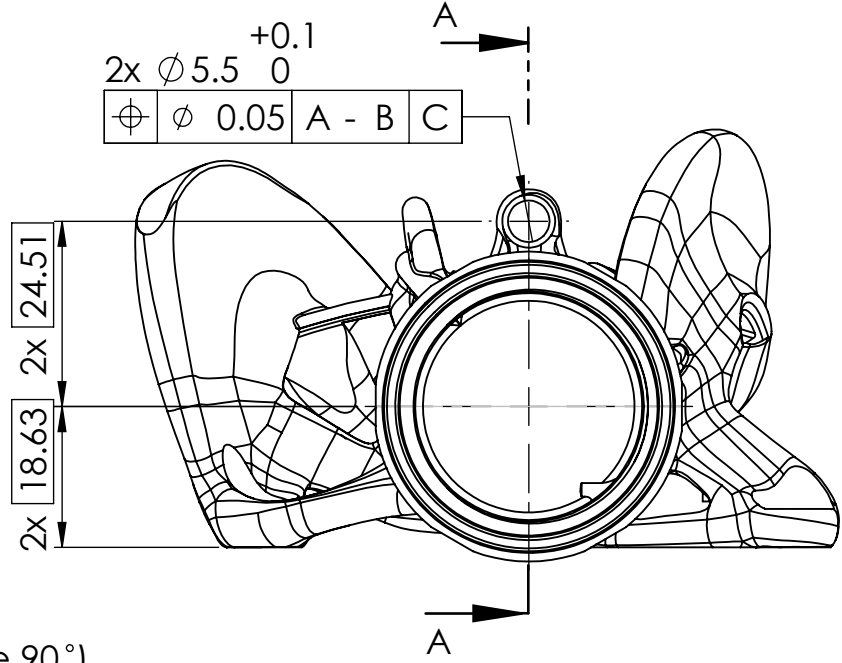
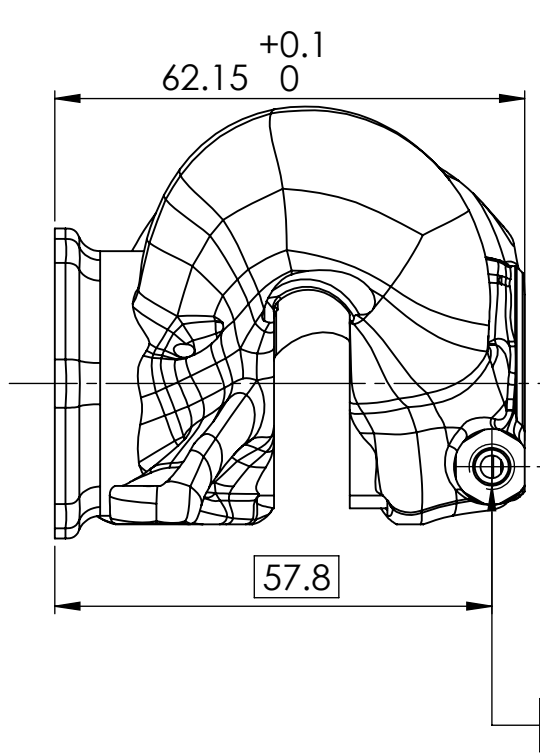
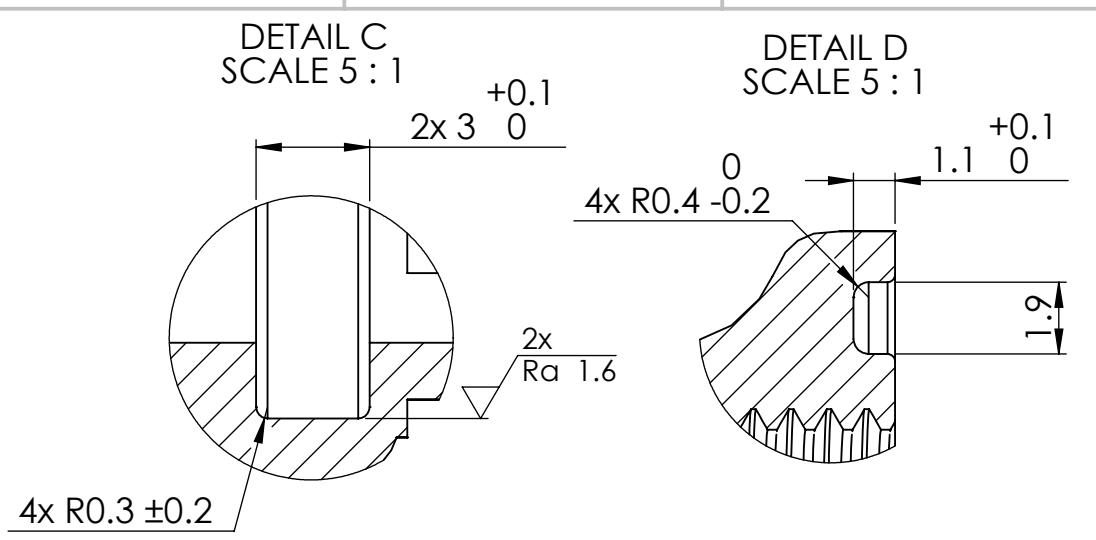
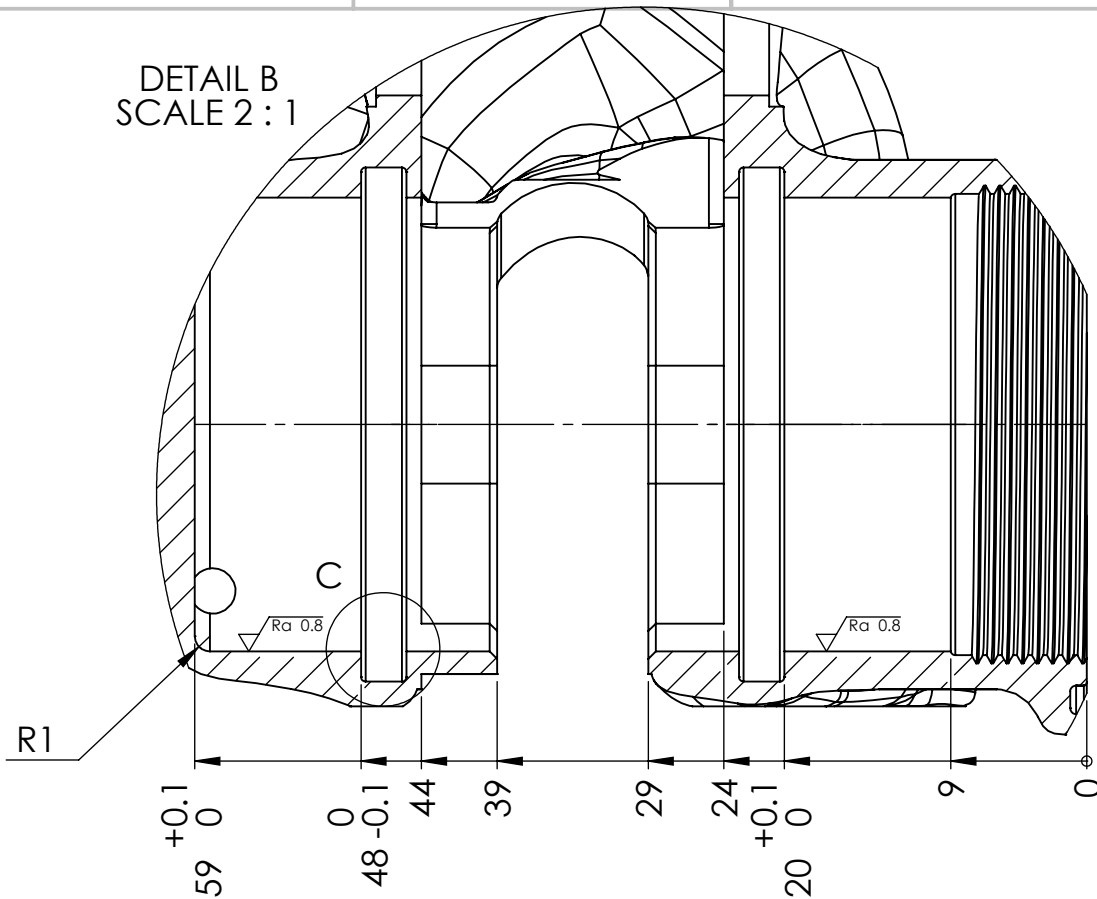
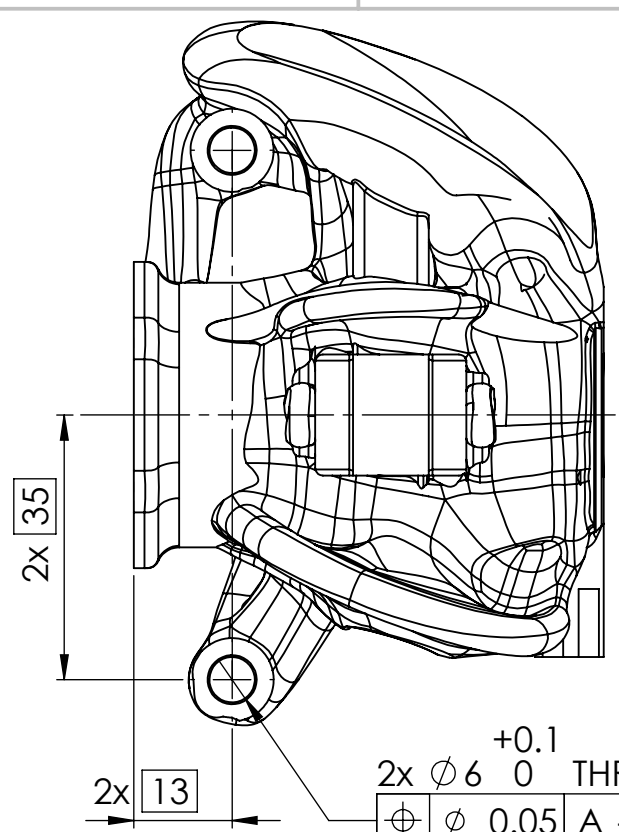


Fig. 4, Housing for wiper A26, A27.

Lead-in chamfer on the rod is designed to suit the rod seal used for surface finish per end of section.

Appendix **F**
Technical Drawings

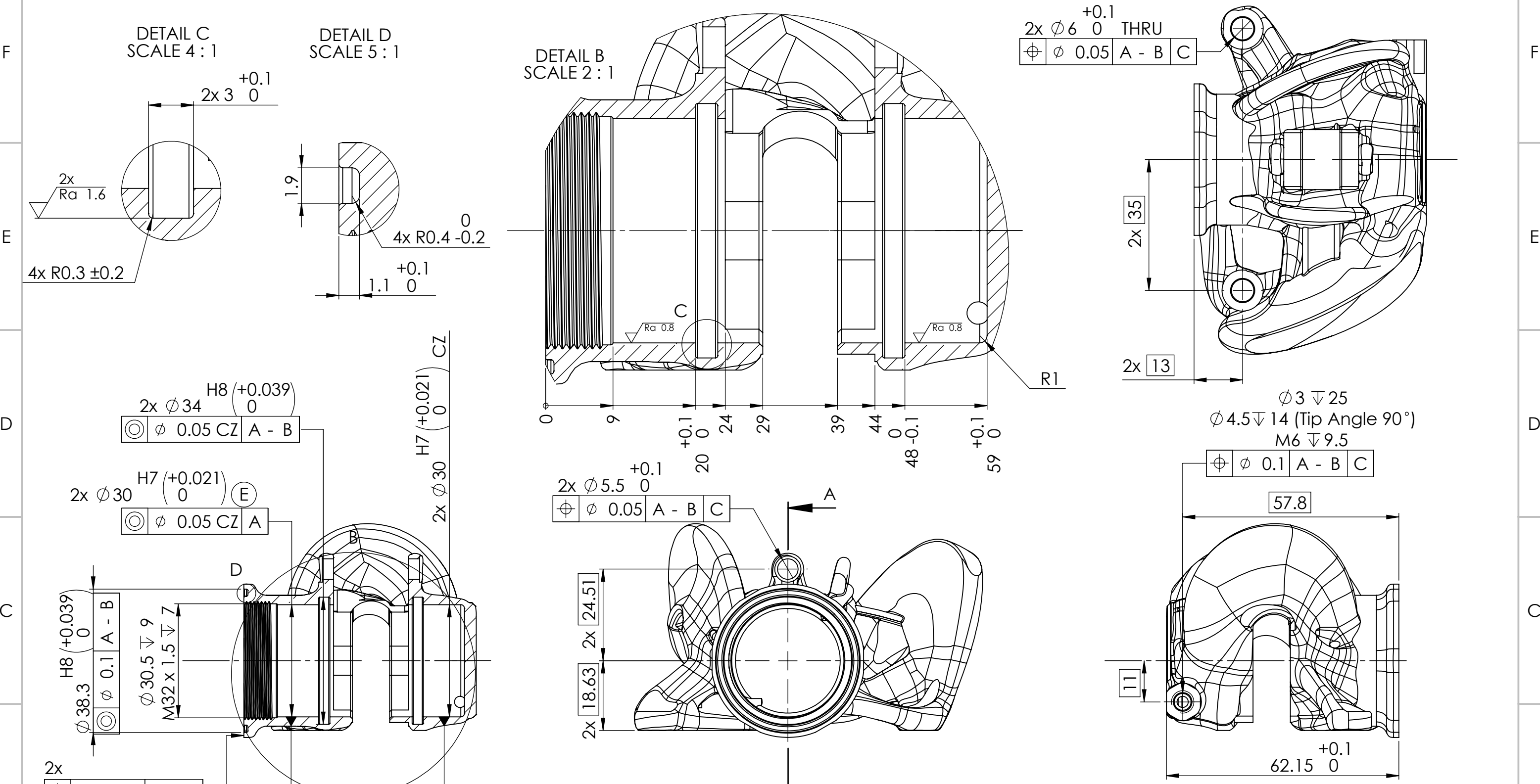


- Notes:**
- 3D model defines nominal shape of part. (For general tolerances, see title field)
 - Part to be delivered clean of cutting fluids, chips and other FOD.

SOLIDWORKS Educational Product. For Instructional Use Only


| | | | | | |
|--|-----|-------------------------------|-------------------------|--|-----------------------------|
| Non-specified geometry should according to 3D CAD model and ISO 8015 | | | | | |
| ROUGHNESS Ra μ m | 3,2 | GENERAL TOL. ISO 2768 - mk | QTY: 1 | BREAK ALL EDGES (R ALT 45°) MAX 0,1 | SIZE A3 |
| Material: Ti6Al4V | | | PROJECTION 1st angle | REVISION A | THREAD TOL 6g/6H ISO R965/1 |
| Design: Mathias Lien | | | Phone: +4797147067 | ALL DIM. INCLUDE SURFACE TREATMENT | |
| Approved: SS | | | Date: 22/02/2020 | | |
| TITLE: S20 Front Left Caliper | | | DWG NO. PRT-18300 | | SCALE: 1:1 |
| Weight: 190.05 g | | | Sheet: 1 / 1 | | |

8 7 6 5 4 3 2 1



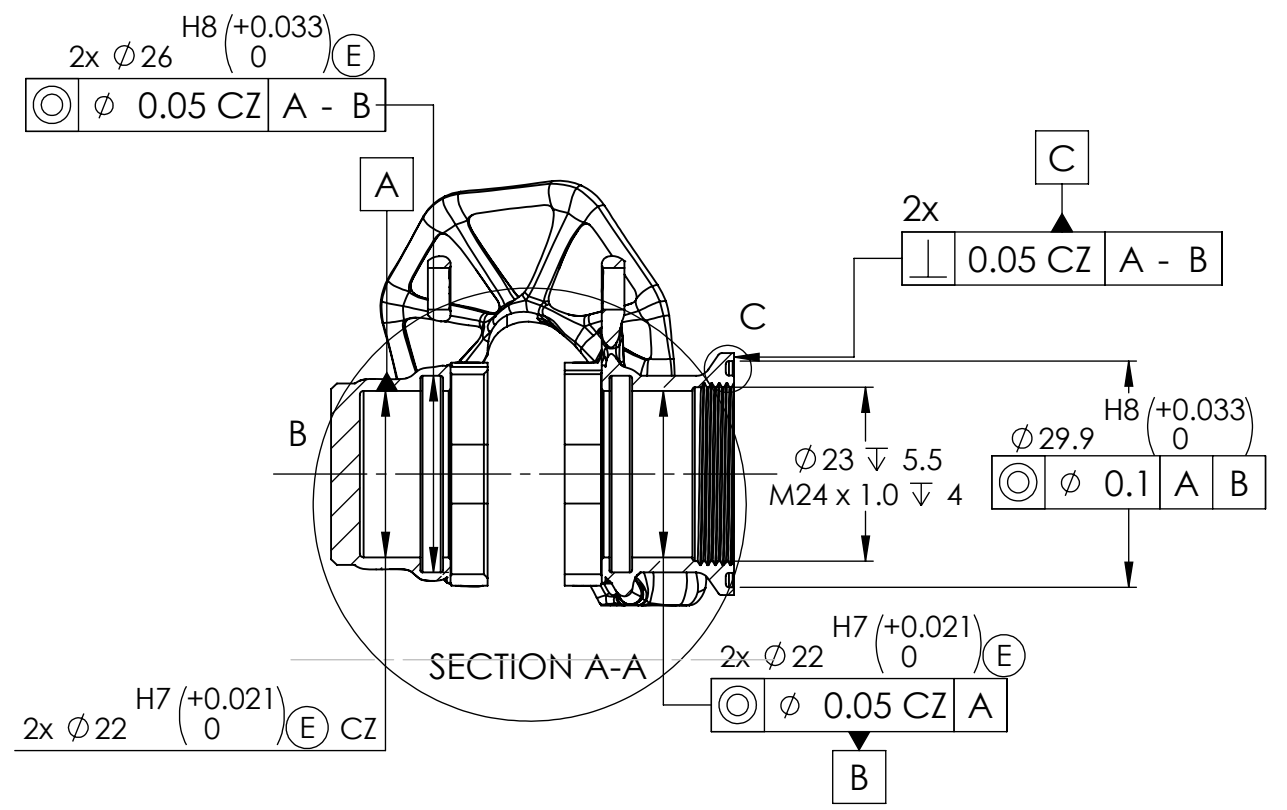
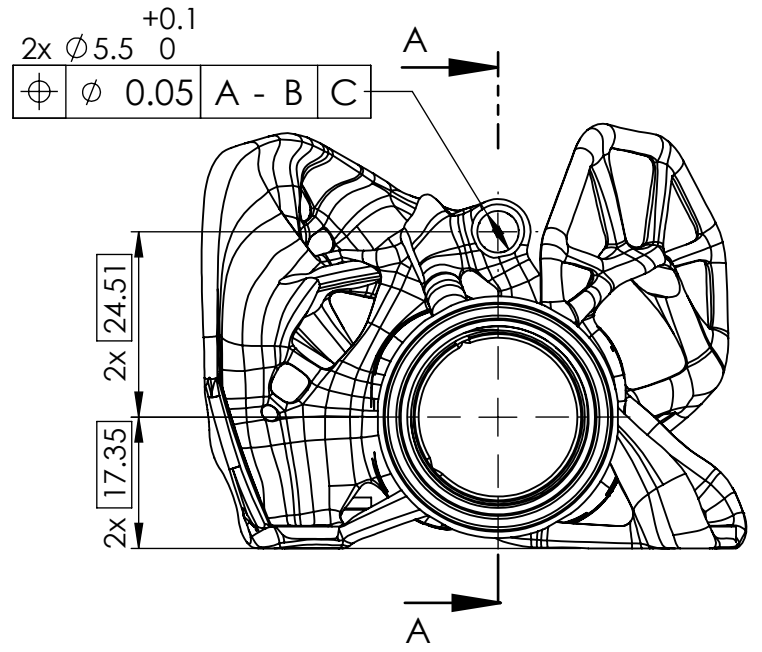
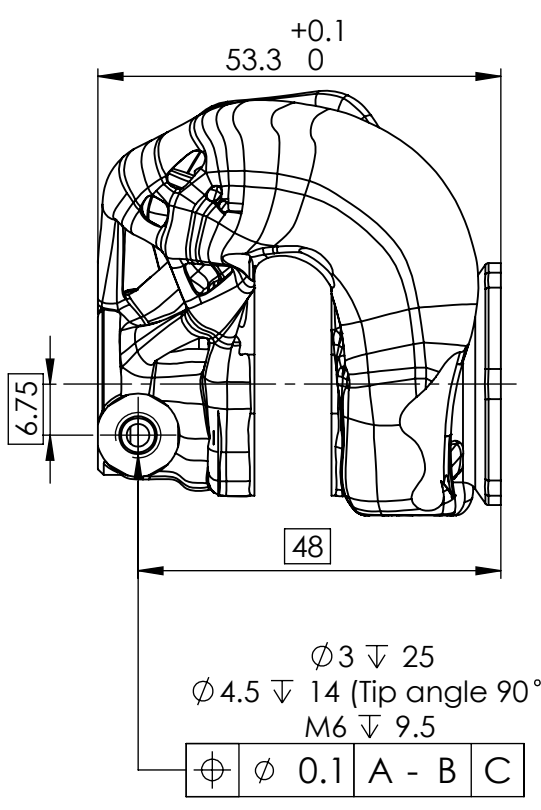
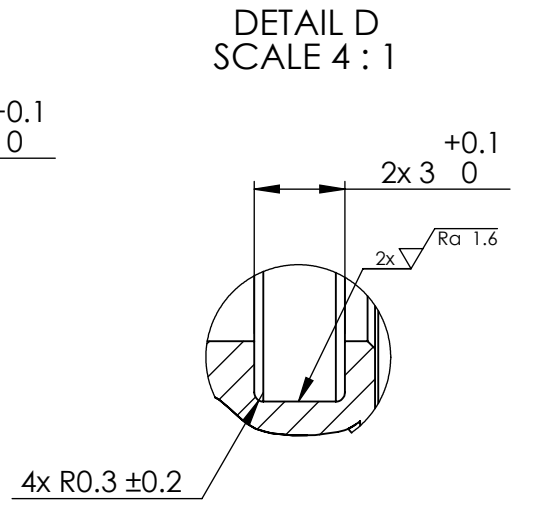
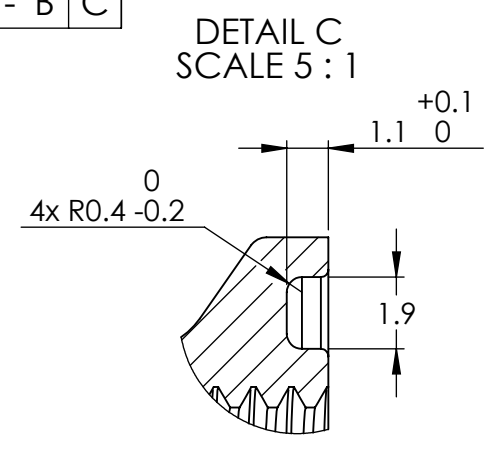
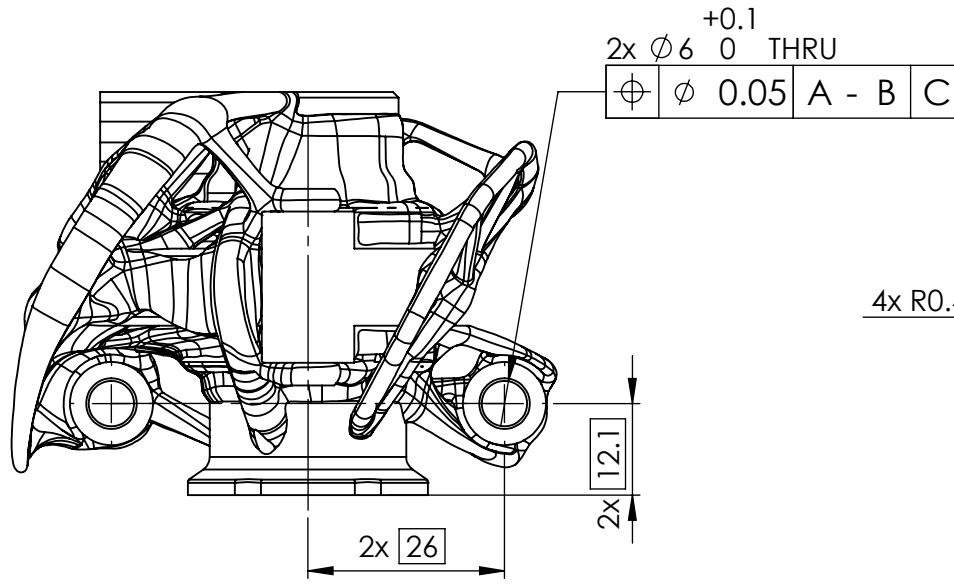
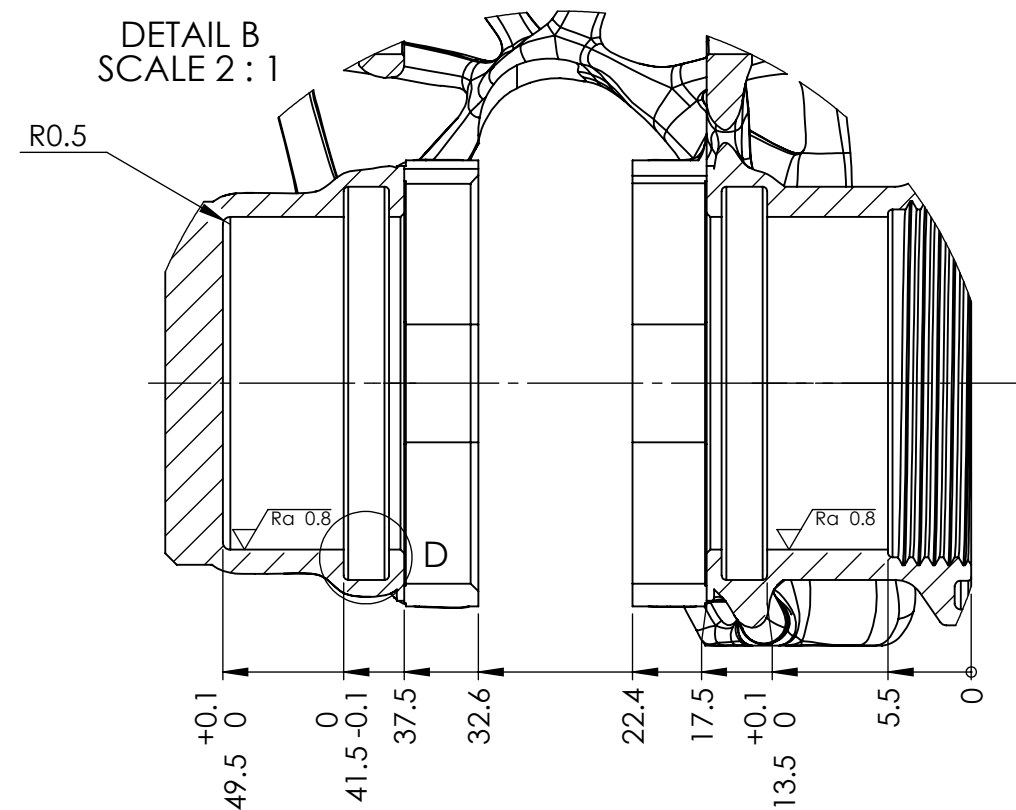
- Notes:**
- 3D model defines nominal shape of part. (For general tolerances, see title field)
 - Part to be delivered clean of cutting fluids, chips and other FOD.

Non-specified geometry should according to 3D CAD model and ISO 8015

| | | | | | | |
|-----------------------------------|-----|-------------------------------|-------------------------|---|------------|---------------|
| ROUGHNESS Ra μm | 3,2 | GENERAL TOL. ISO 2768 - mk | QTY: 1 | BREAK ALL EDGES (R ALT 45°) MAX 0,1 | SIZE A3 | REVISION A |
| Material: Ti6Al4V | | | PROJECTION 1st angle | ALL DIM. INCLUDE SURFACE TREATMENT | | |
| Design: Mathias Lien | | | Phone: +4797147067 |  | | |
| Approved: Yes | | | Date: 22/02/2020 | | | |
| TITLE: S20 Front Right Caliper | | | | DWG NO. 1 | | |
| Weight: 190.05g | | | | SCALE: 1:1 | | Sheet: 1 / 1 |

SOLIDWORKS Educational Product. For Instructional Use Only

8 7 6 5 4 3 2 1

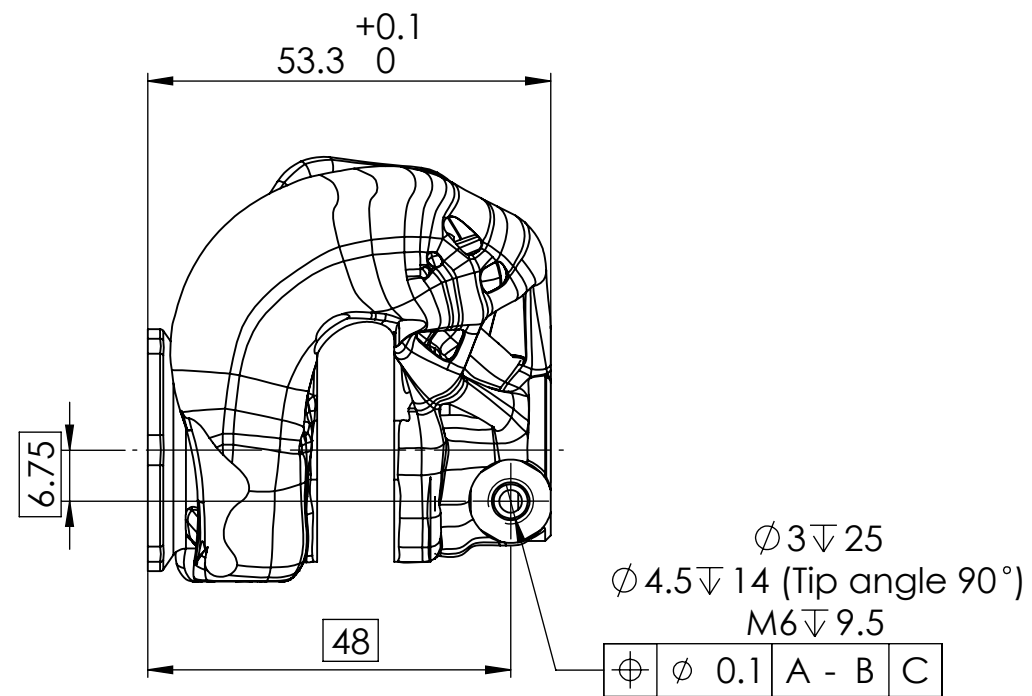
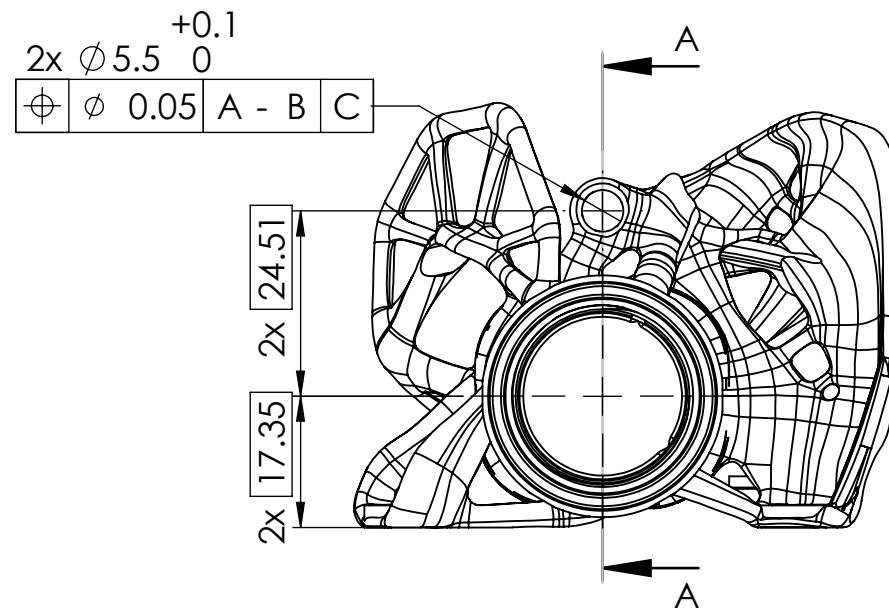
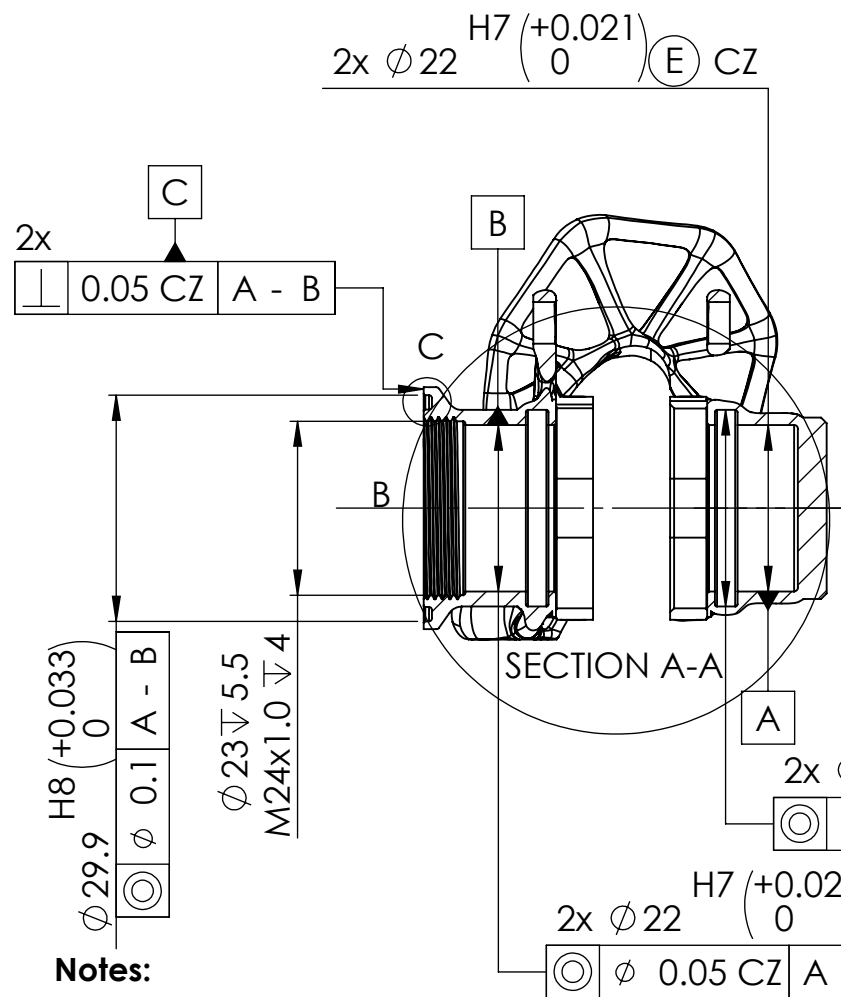
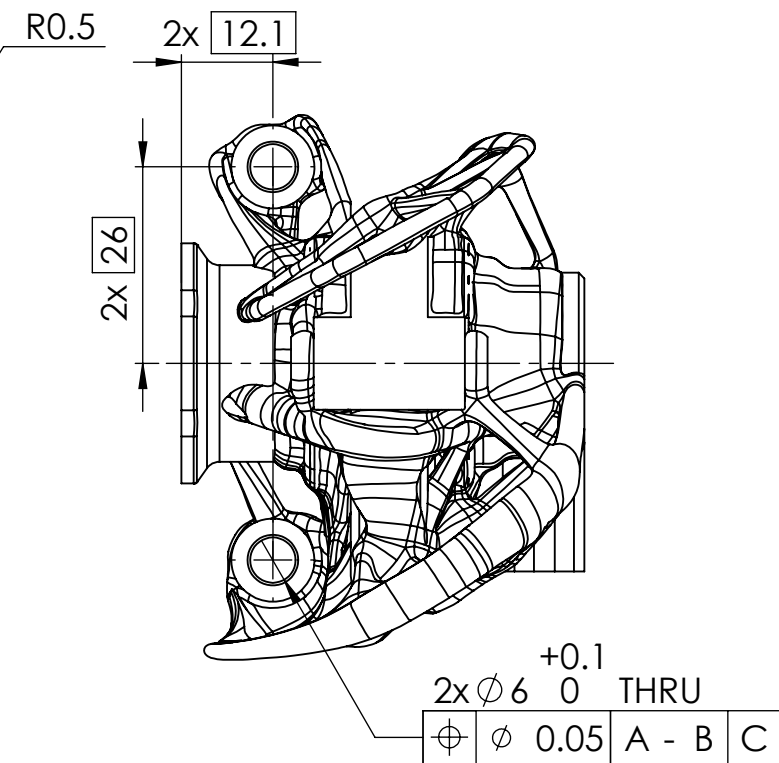
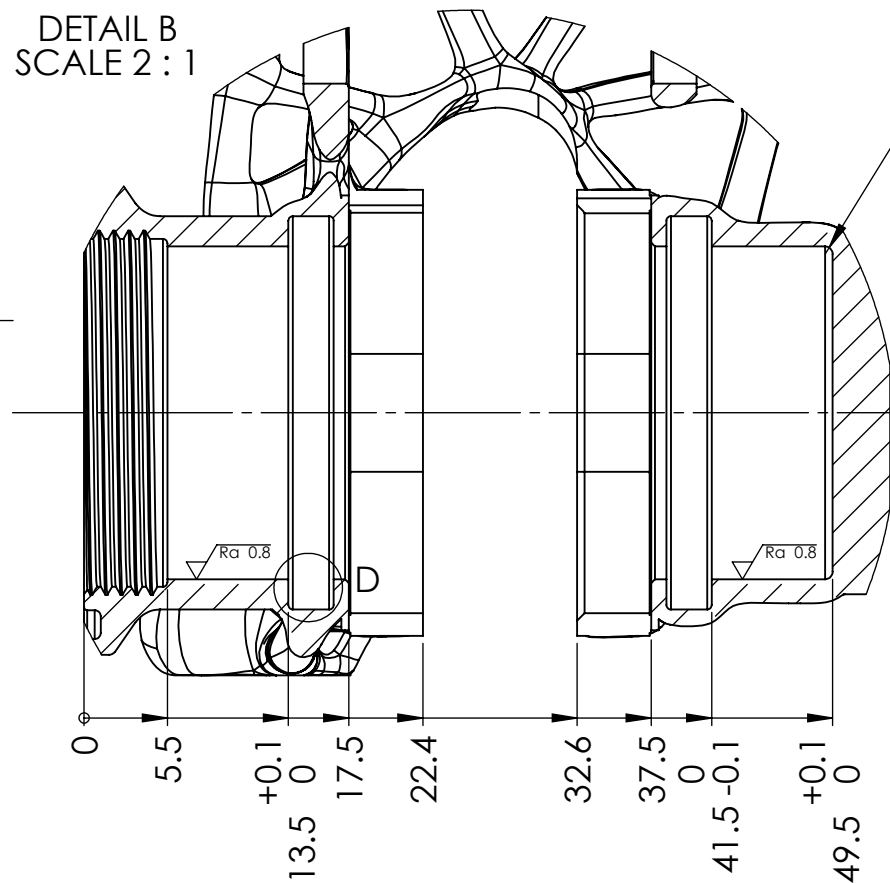
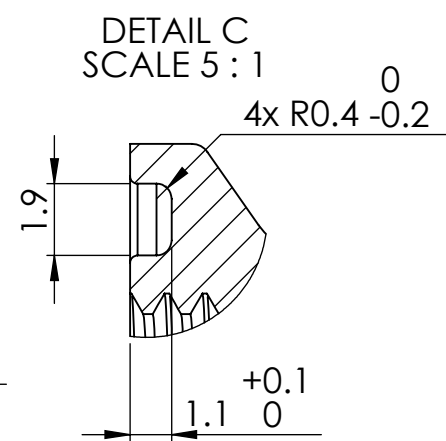
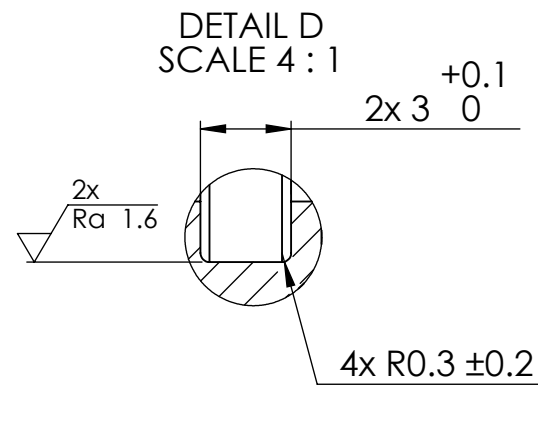


- Notes:**
- 3D model defines nominal shape of part. (For general tolerances, see title field)
 - Part to be delivered clean of cutting fluids, chips and other FOD.

SOLIDWORKS Educational Product. For Instructional Use Only

| | | | | | |
|--|-----|-------------------------------|-------------------------|--|--------------|
| Non-specified geometry should according to 3D CAD model and ISO 8015 | | | | | |
| ROUGHNESS Ra µm | 3,2 | GENERAL TOL. ISO 2768 - mk | QTY: 2 | BREAK ALL EDGES (R ALT 45°) MAX 0,1 | SIZE A3 |
| Material: Ti6Al4V | | | PROJECTION 1st angle | REVISION A | |
| Design: Mathias Lien | | Phone: +4797147067 | | THREAD TOL 6g/6H ISO R965/1 | |
| Approved: SS | | Date: 22/02/2020 | | ALL DIM. INCLUDE SURFACE TREATMENT | |
| TITLE: S20 Rear Left Caliper | | | DWG NO. PRT-18548 | | |
| Weight: 85 g | | | SCALE: 1:1 | | Sheet: 1 / 2 |





Notes:

- 3D model defines nominal shape of part. (For general tolerances, see title field)
- Part to be delivered clean of cutting fluids, chips and other FOD.

SOLIDWORKS Educational Product. For Instructional Use Only

Non-specified geometry should according to 3D CAD model and ISO 8015

| | | | | | |
|----------------------------------|-------------------------------|--------|--|------------|---------------|
| ROUGHNESS Ra μm | GENERAL TOL. ISO 2768 - mk | QTY: 2 | BREAK ALL EDGES (R ALT 45°) MAX 0,1 | SIZE A3 | REVISION A |
| Material: Ti6Al4V | | | THREAD TOL 6g/6H ISO R965/1 | | |
| Design: Mathias Lien | | | ALL DIM. INCLUDE SURFACE TREATMENT | | |
| Approved: SS | | | | | |
| TITLE: S20 Rear Right Caliper | | | | | |
| Weight: 85 g | | | DWG NO. 2 | | |
| | | | SCALE:1:1 | | Sheet: 1 / 1 |

6 5 4 3 2 1

D

C

B

A

D

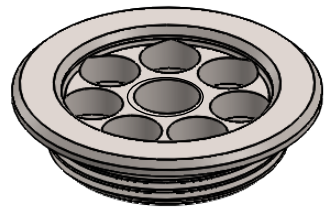
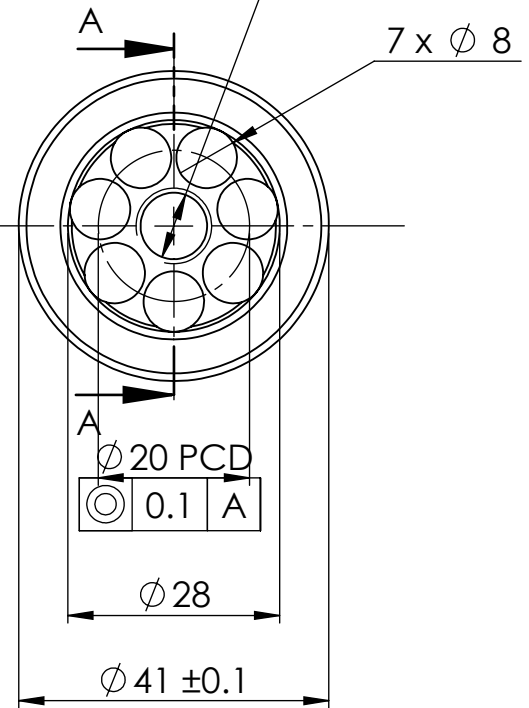
C

B

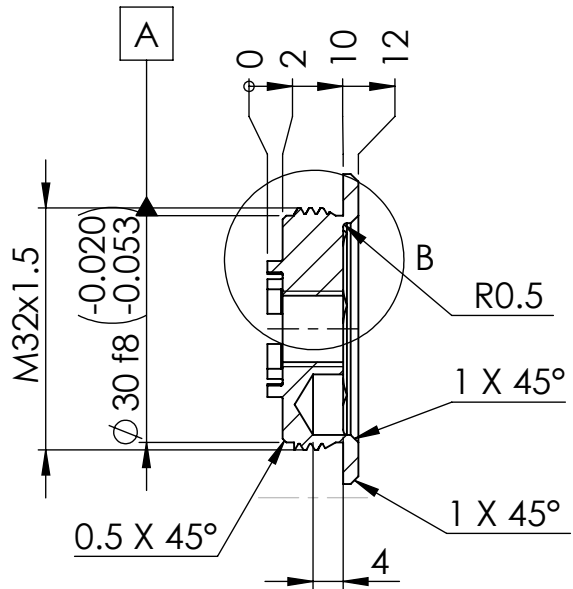
A

M10x1.25 THRU ALL

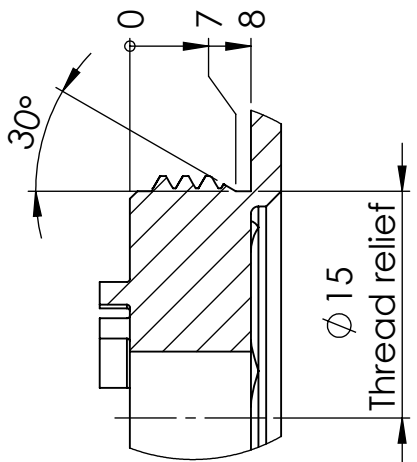
⊙ 0.1 A



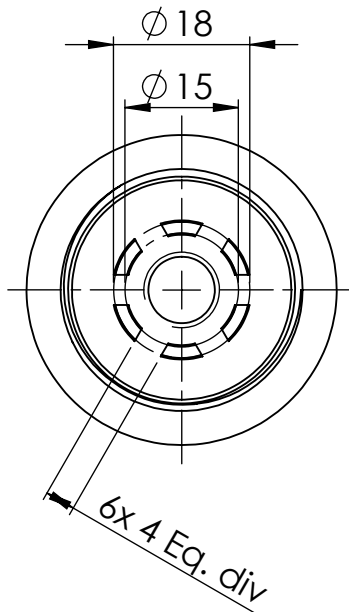
SOLIDWORKS Educational Product. For Instructional Use Only



SECTION A-A



DETAIL B
SCALE 2 : 1

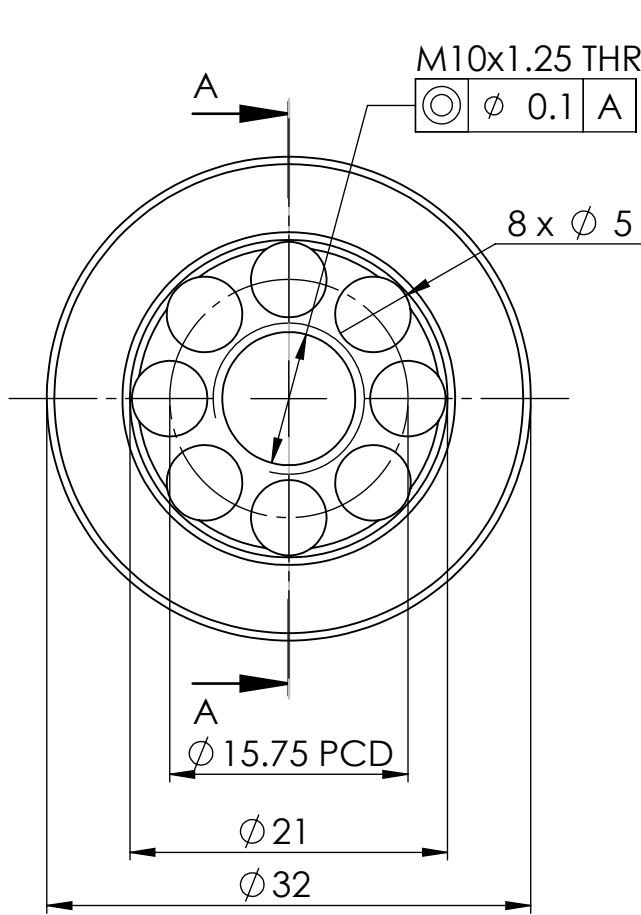


Notes:

- 3D model defines nominal shape of part. (For general tolerances, see title field)
- Part to be delivered clean of cutting fluids, chips and other FOD.

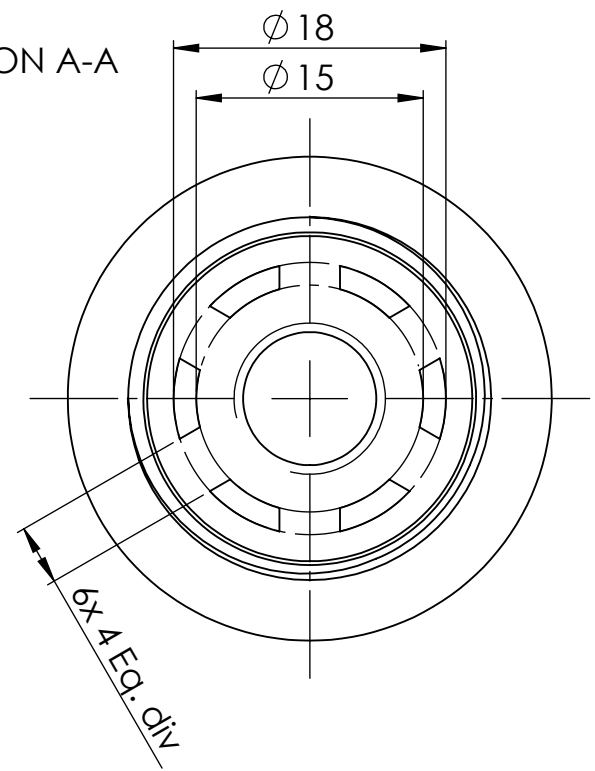
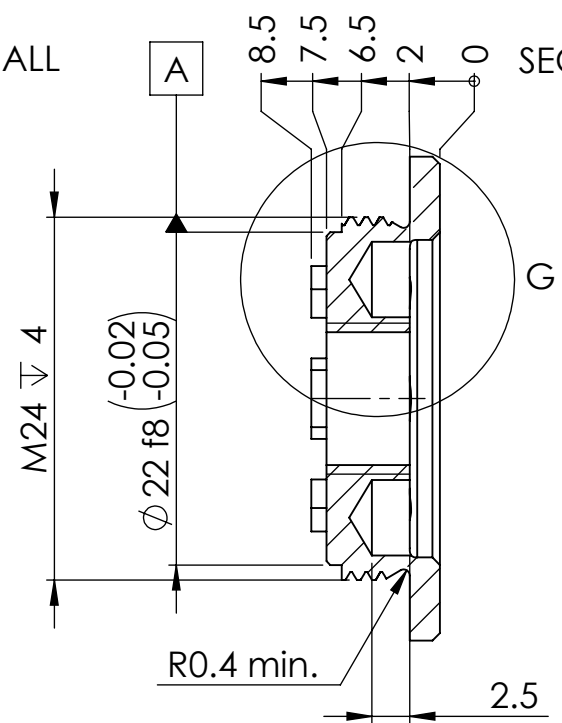
| | | | |
|--|-------------------------------|-------------------------|---|
| Non-specified geometry should according to 3D CAD model and ISO 8015 | | | |
| ROUGHNESS Ra μ m 3,2 | WEIGHT: 23 g QTY: 2 | REVISION: SIZE: A4 | THREAD TOL 6g/6H ISO R965/1 ALL DIM. INCLUDE SURFACE TREATMENT |
| BREAK ALL EDGES (R ALT 45°) MAX 0,1 | GENERAL TOL. ISO 2768 - mk | PROJECTION 1st angle | |
| Material: Ti-6Al-4V Solution treated and aged (SS) | | | |
| Date: 19/05/2020 | | | Phone: |
| Design: Mathias Lien | | | SCALE: 1:1 Sheet: 1 / 1 |
| Approved: Not Approved | | | DWG NO.: PRT-11461 |
| TITLE: S20 Caliper End Cap | | | |

6 5 4 3 2 1

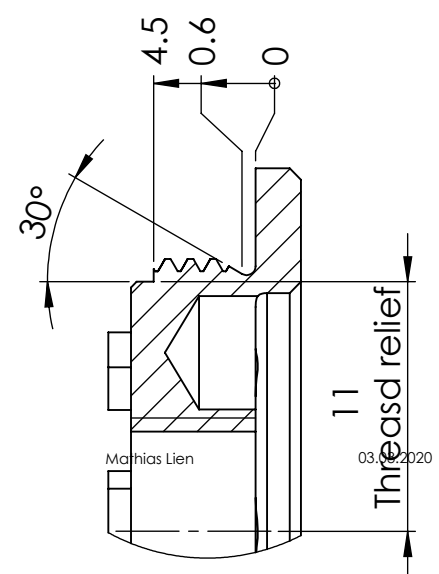


M10x1.25 THRU ALL

$\phi 0.1$ A

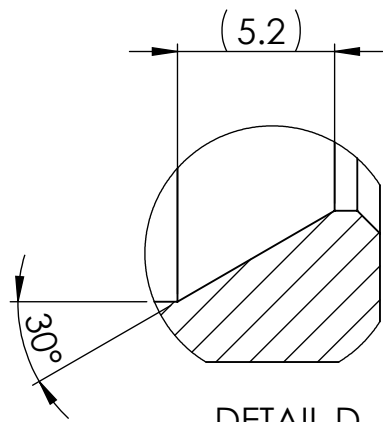
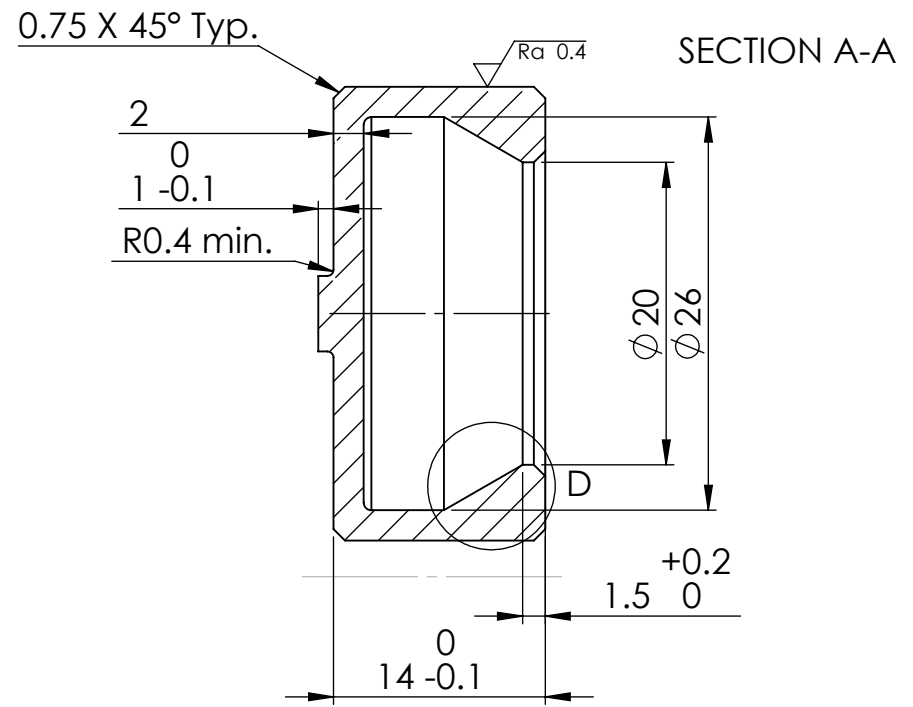
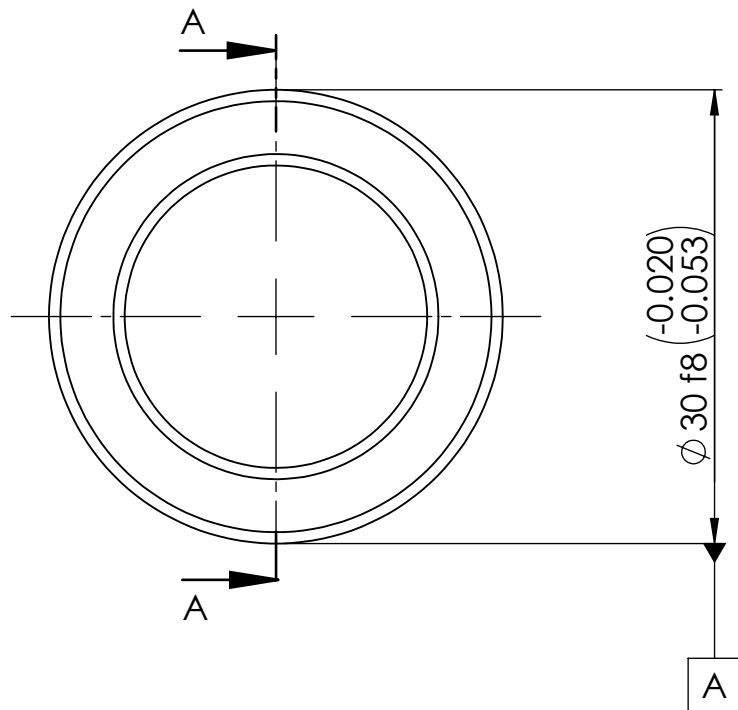


- Notes:**
- 3D model defines nominal shape of part. (For general tolerances, see title field)
 - Part to be delivered clean of cutting fluids, chips and other FOD.

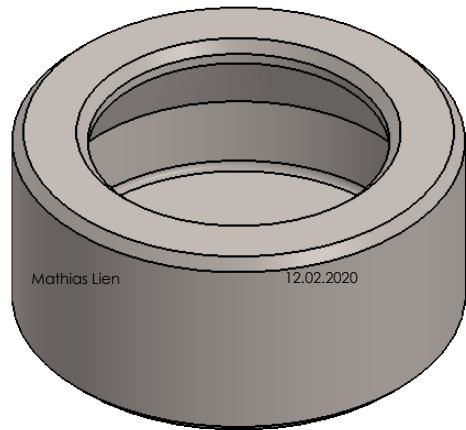


DETAIL G
SCALE 3 : 1

| | | | |
|--|-------------------------------|-------------------------|---|
| Non-specified geometry should according to 3D CAD model and ISO 8015 | | | |
| ROUGHNESS Ra μ m 3,2 | WEIGHT: QTY: | REVISION: SIZE: A4 | THREAD TOL 6g/6H ISO R965/1 ALL DIM. INCLUDE SURFACE TREATMENT |
| BREAK ALL EDGES (R ALT 45°) MAX 0,1 | GENERAL TOL. ISO 2768 - mk | PROJECTION 1st angle | |
| Material: | Date: 19/05/2020 | | |
| Design: Mathias Lien | Approved: Not Approved | Phone: | SCALE:2:1 Sheet: 1 / 1 |
| TITLE:S20 Rear Caliper End Cap | | DWG NO.:PRT-17626 | |



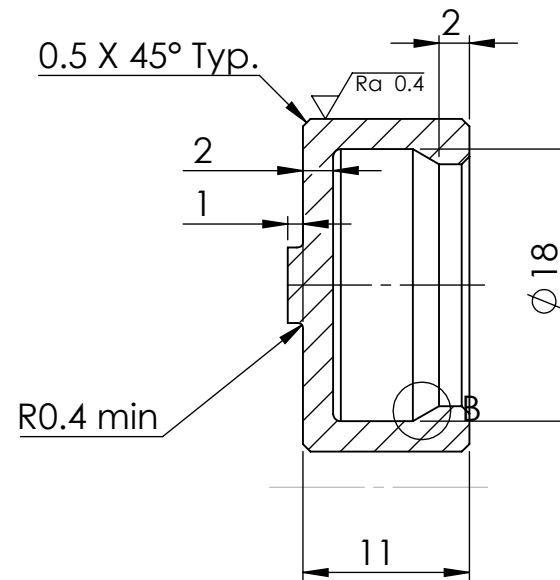
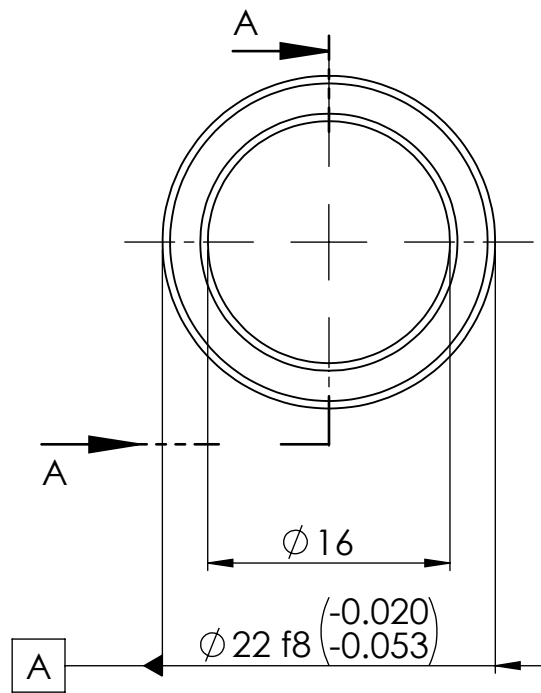
DETAIL D
SCALE 4 : 1



Notes:

- 3D model defines nominal shape of part. (For general tolerances, see title field)
- Part to be delivered clean of cutting fluids, chips and other FOD.

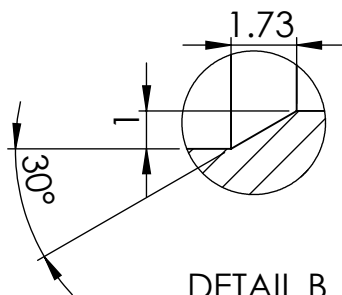
| | | | |
|--|-------------------------------|-------------------------|---|
| Non-specified geometry should according to 3D CAD model and ISO 8015 | | | |
| ROUGHNESS Ra μm 3,2 | WEIGHT: QTY: | REVISION: SIZE: A4 | THREAD TOL 6g/6H ISO R965/1 ALL DIM. INCLUDE SURFACE TREATMENT |
| BREAK ALL EDGES (R ALT 45°) MAX 0,1 | GENERAL TOL. ISO 2768 - mk | PROJECTION 1st angle | |
| Material: | | | |
| Date: 19/05/2020 | | Phone: | |
| Design: Mathias Lien | | SCALE:2:1 Sheet: 1 / 1 | |
| Approved: Not Approved | | DWG NO.: PRT-14923 | |
| TITLE: S20 Caliper Piston_Ø30_Ti64 | | | |



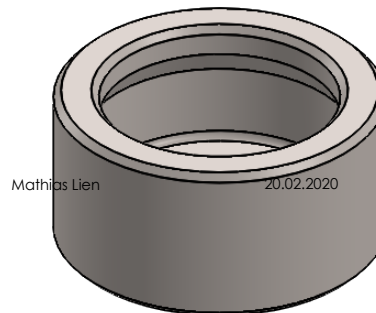
SECTION A-A

Notes:

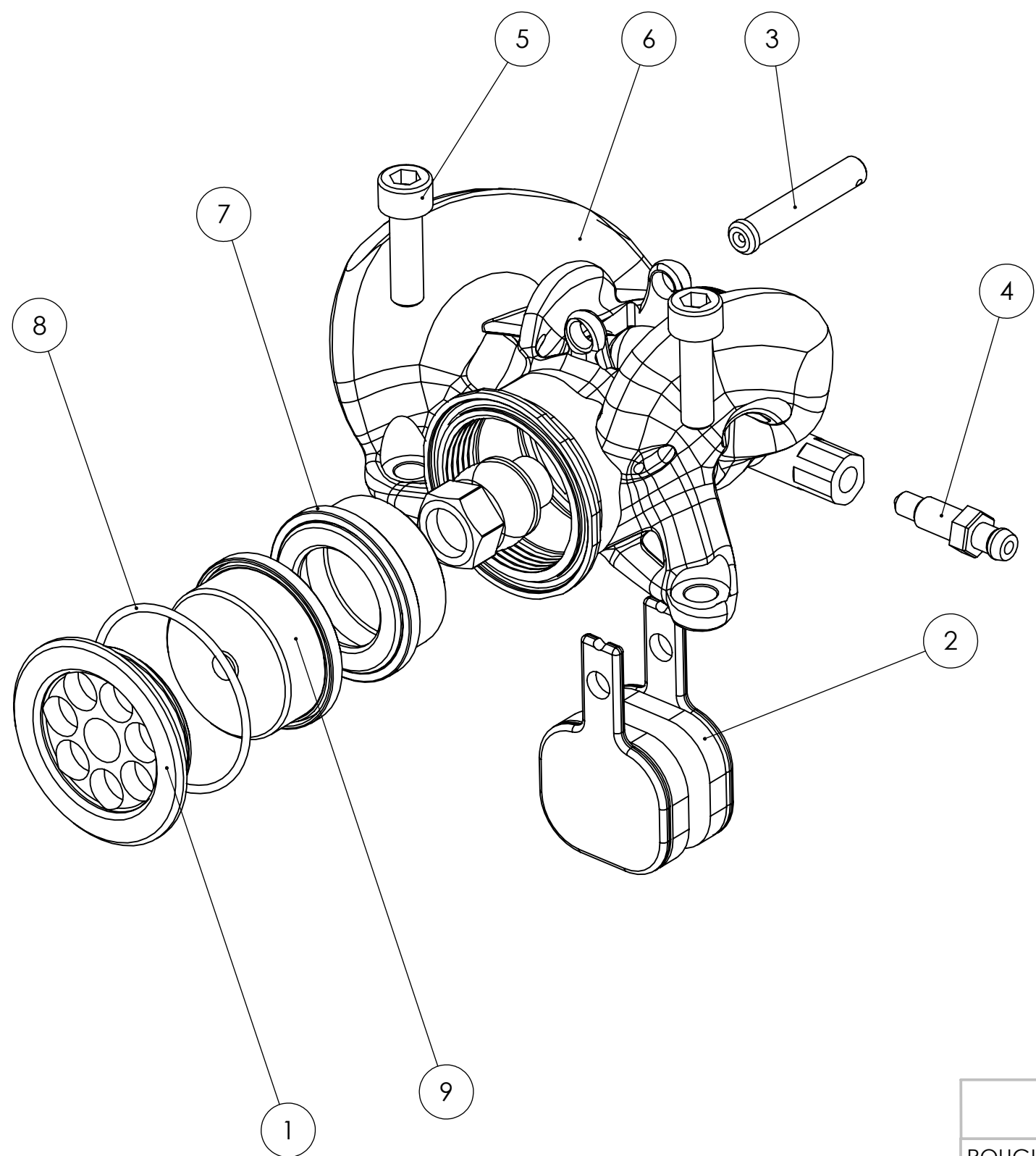
- 3D model defines nominal shape of part. (For general tolerances, see title field)
- Part to be delivered clean of cutting fluids, chips and other FOD.



DETAIL B
SCALE 5 : 1



| | | | |
|--|-------------------------------|-------------------------|---|
| Non-specified geometry should according to 3D CAD model and ISO 8015 | | | |
| ROUGHNESS Ra μm 3,2 | WEIGHT: QTY: | REVISION: SIZE: A4 | THREAD TOL 6g/6H ISO R965/1 ALL DIM. INCLUDE SURFACE TREATMENT |
| BREAK ALL EDGES (R ALT 45°) MAX 0,1 | GENERAL TOL. ISO 2768 - mk | PROJECTION 1st angle | |
| Material: | | | |
| Date: 19/05/2020 | | Phone: | |
| Design: Mathias | | SCALE:2:1 | Sheet: 1 / 1 |
| Approved: Not Approved | | DWG NO.: PRT-17557 | |
| TITLE: S20 Caliper $\phi 22_{Ti64}$ | | | |



| ITEM NO. | PART NUMBER | QTY. |
|----------|----------------------------|------|
| 1 | S20 Caliper End Cap | 1 |
| 2 | ISR Brake Pad | 2 |
| 3 | S20 Caliper Pad Pin | 1 |
| 4 | S20 M6x1 27mm bleed nipple | 1 |
| 5 | Screw - DIN912 M6 x 20 | 2 |
| 6 | S20 Front Caliper Housing | 1 |
| 7 | S20 Lip Seal | 2 |
| 8 | S20 BS-208 O-ring | 1 |
| 9 | S20 Caliper Piston Ø30 | 2 |

Notes:

- 3D model defines nominal shape of part. (For general tolerances, see title field)
- Part to be delivered clean of cutting fluids, chips and other FOD.

SOLIDWORKS Educational Product. For Instructional Use Only

| Non-specified geometry should according to 3D CAD model and ISO 8015 | | | | |
|--|-----|-------------------------------|--------|--|
| ROUGHNESS Ra µm | 3,2 | GENERAL TOL. ISO 2768 - mk | QTY: 1 | BREAK ALL EDGES (R ALT 45°) MAX 0,1 |
| | | | | SIZE A3 |
| | | | | REVISION |
| | | | | THREAD TOL 6g/6H ISO R965/1 |
| Material: | | PROJECTION 1st angle | | ALL DIM. INCLUDE SURFACE TREATMENT |
| Design: Mathias Lien | | Phone: +4797147067 | | |
| Approved: | | Date: 19/12/2020 | | |
| TITLE: S20 Front Caliper Assembly | | | | DWG NO. ASS-2982 |
| Weight: 280.86 g | | | | SCALE: 1:5 |
| | | | | Sheet: 1 / 1 |

8

7

6

5

4

3

2

1

F

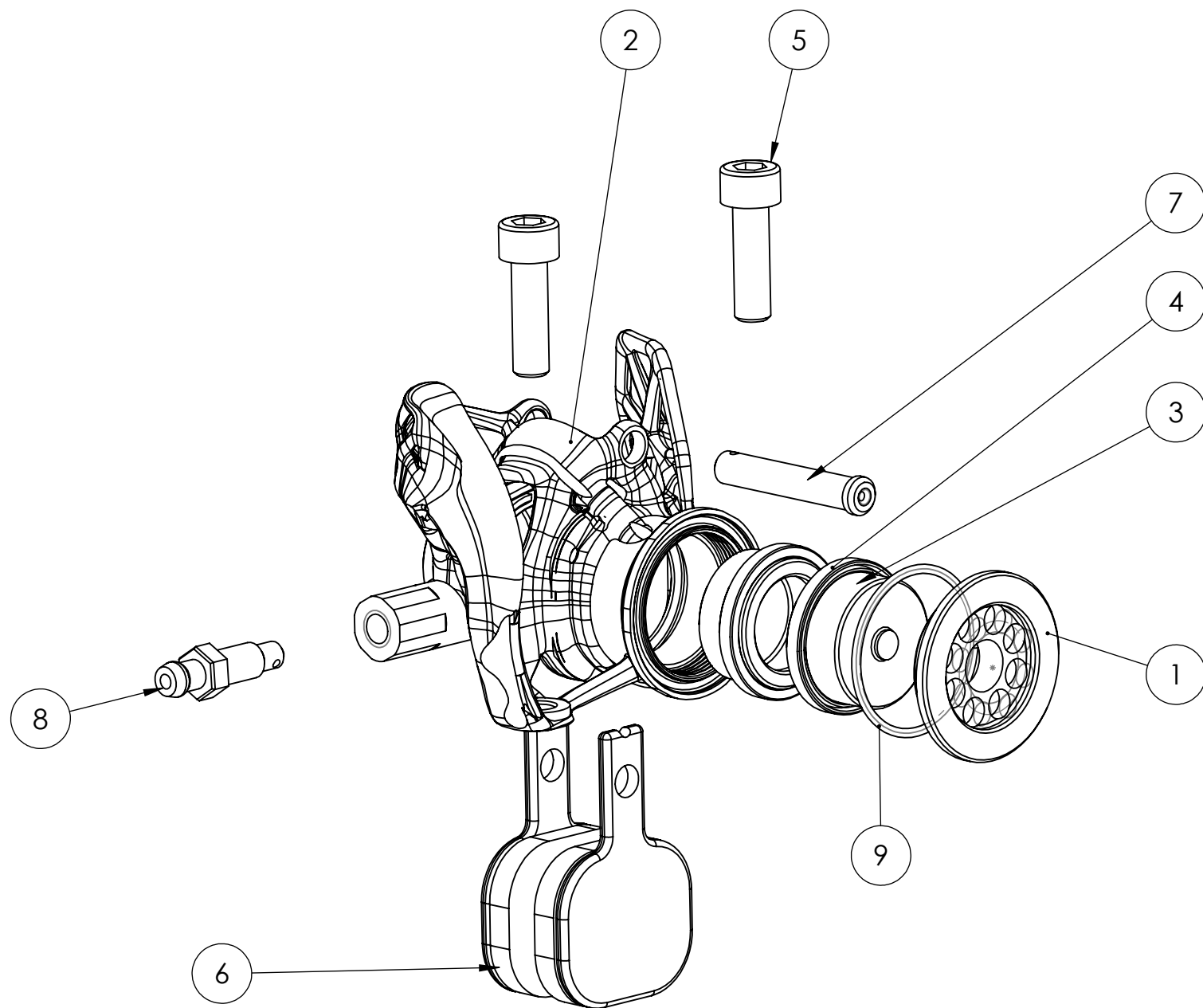
E

D

C

B

A




| ITEM NO. | PART NUMBER | QTY. |
|----------|------------------------------|------|
| 1 | S20 Rear Caliper End Cap | 1 |
| 2 | S20 Rear Caliper Housing | 1 |
| 3 | S20 Caliper Piston Ø22 | 2 |
| 4 | S20 Rear Caliper Lipseal Ø22 | 2 |
| 5 | Screw - DIN 912 M6 x 20 | 2 |
| 6 | ISR Brake Pad | 2 |
| 7 | S20 Caliper Pad Pin | 1 |
| 8 | S20 M6x1 27mm bleed nipple | 1 |
| 9 | S20 O-ring Ø26 | 1 |

Notes:

- 1. 3D model defines nominal shape of part. (For general tolerances, see title field)
- 2. Part to be delivered clean of cutting fluids, chips and other FOD.

SOLIDWORKS Educational Product. For Instructional Use Only

Non-specified geometry should according to 3D CAD model and ISO 8015

| | | | | | | |
|-------------------------------------|-----|-------------------------------|-------------------------|---|------------|-------------|
| ROUGHNESS Ra µm | 3,2 | GENERAL TOL. ISO 2768 - mk | QTY: 2 | BREAK ALL EDGES (R ALT 45°) MAX 0,1 | SIZE A3 | REVISION: A |
| Material: Ti6Al4V | | | PROJECTION 1st angle | THREAD TOL 6g/6H ISO R965/1 | | |
| Design: Mathias Lien | | | Phone: +4797147067 | ALL DIM. INCLUDE SURFACE TREATMENT | | |
| Approved: | | | Date:19/05/2020 |  | | |
| TITLE: S20 Rear Caliper Assembly | | | DWG NO. ASS-3993 | | | |
| Weight: 140 g | | | SCALE:1:2 | Sheet: 1 / 1 | | |

8

7

6

5

4

3

2

1

B

A

